Environmental Science: Atmospheres

ROYAL SOCIETY OF CHEMISTRY

PAPER

View Article Online
View Journal | View Issue

Cite this: *Environ. Sci.: Atmos.*, 2025, **5**, 1243

Intra-city particulate elemental characteristics and variabilities in Jakarta

Driejana, *[a] Novi Kartika Sari,[bd] Muhayatun Santoso[c] and Dyah Dwiana Lestiani[c]

Jakarta has experienced a particulate pollution problem in the last few decades. Our study aimed to investigate particulate spatial variability and identify the associated sources in more detail by measuring their composition in Jakarta at three sites in a north–south transect. We collected the mass using the Dichotomous Gent SFU and analysed the elemental concentration with a Smoke Stain Reflectometer and ED-XRF. Principal Component Analysis (PCA), correlation, and Conditional Bivariate Probability Function (CBPF) techniques were used to reveal the element's source attribution probabilities and their directional strengths. Black carbon (BC) and sulphur (S) were the major contributors to PM2.5 but not always to coarse particles. Motor vehicle fuel was a significant source of sulphur in most areas. Multiple-site data analyses reveal that in the city centre, traffic congestion was the main source of BC, while in South Jakarta, BC primarily originated from open waste/biomass burning. However, in North Jakarta, CBPF also suggested industrial coal and vessel diesel oil from the direction of the port as probable sulphur sources. While local sources dominated, the fine and coarse particle CBPFs demonstrated that some elements arrived from out-of-border sources during higher wind speed events. Long-distance anthropogenic and natural sources might include industries in the neighbouring cities and fumarolic emissions from the volcanic terrains in southern Jakarta. These results showed diverse sources and composition of PM in Jakarta's north-to-south transect. The large proportion of calm wind underscores the contrasted local sources' contribution to each site, leading to the apparent spatial and source variability within sites.

Received 16th May 2025
Accepted 19th September 2025

DOI: 10.1039/d5ea00059a

rsc.li/esatmospheres

Environmental significance

Particulate matter (PM) is one of the indicators of SDGs for cities and human settlements. It is a significant air quality problem in Jakarta that severely affects public health. PM originates from a complex mixture of chemical compounds from many sources, often exceeding the NAAQS, particularly in the dry season. Fine and coarse particles can vary spatially in their total concentration and composition. Some elements in PM control approaches require lengthy coordination of authorities at several levels of the chain of command. Therefore, understanding local spatial variability of PM, including its chemical composition and associated sources, is the key factor that would empower the local authorities to opt for directly executable alternative actions to control specific sources at the local level.

1 Introduction

The United Nations has confirmed its commitment to the Sustainable Development Goal (SDG) targets 3.9 and 11.6 of healthy air quality to achieve sustainable cities. Air pollution, more specifically particulate matter, was declared as the first risk factor for the Global Burden of Diseases (GBD) in the Sixty-eighth World Health Assembly.[1] Particulate pollution is an emerging concern in Indonesia, where GBD study ranked ambient PM2.5 as the seventh mortality risk factor.[2]

PM10 and PM2.5 with various chemical and organic compounds are significant air pollutants found in urban environments.[3–5] The impacts of PM10 and PM2.5 on human health and climate change are well established.[2,6] PM10 and PM2.5 cause damage to human DNA, pulmonary inflammation, ischemic heart disease, lower respiratory infection, lung cancer, and type 2 diabetes mellitus.[2,7–9] PM2.5 effects on health are more severe in sensitive populations.[10]

Jakarta, the capital of Indonesia, is a province comprising six city administrations in the northwestern corner of Java Island, Indonesia. It is facing a significant challenge due to high population density. The Jakarta Bay in the north borders the Java Sea, and the cities of Bogor, Depok, Tangerang, South

[a]*Air and Waste Management Research Group, Faculty of Civil and Environmental Engineering, Institut Teknologi Bandung, Jl. Ganesa 10, Bandung 40132, Indonesia. E-mail: driejana@itb.ac.id*

[b]*Environmental Engineering Graduate Programme, Faculty of Civil and Environmental Engineering, Institut Teknologi Bandung, Jl. Ganesa 10, Bandung 40132, Indonesia*

[c]*Research Organization for Nuclear Energy, National Research and Innovation Agency BRIN, Jl. Tamansari 71 Bandung, Indonesia*

[d]*Department , of Environmental Engineering, Institut Teknologi Sumatera, Jl. Terusan Ryacudu, Lampung Selatan 35365, Indonesia*

Tangerang, and Bekasi, flank and add to the province to form a Greater Jakarta conurbation.

Indonesia is influenced by El Niño-southern oscillation (ENSO), divided into three climatic rainfall regions of A, B, and C. Jakarta is in the climate region A that is affected by two seasons (monsoons). The northwest monsoon is from November to March, while the dry southeast monsoon usually arrives from May to September.[11] Due to this ENSO oscillation, Jakarta's climate is tropical. The typical westerly wind prevails in the dry season from April to September, while easterly wind occurs in the wet season from October to March.[12] The temperature is warm, ranging from (23–36.6) °C, and the average humidity is 73.8%, ranging between (35 – 95) %.[13]

Jakarta, a city with a population of almost 10.5 million in 2018, is witnessing continuous growth, with the current total exceeding 11 million. The number of registered vehicles, a staggering 20.5 million in 2018, was nearly double the population, indicating an average annual growth of 1.07 million. Notably, motorcycles, accounting for approximately 75% of the total,[14] are a dominant mode of transportation in the city. The daily number of operating vehicles could be higher, as commuters come from the surrounding cities. Residents, buildings, and roads cover over 85% of Jakarta's area, reflecting the high population density and the resulting urban sprawl. This density poses significant challenges to the city's infrastructure and environment. Small and large-scale industries are present in certain areas, primarily concentrated in North Jakarta.

Jakarta is facing significant challenges in managing air quality.[15–19] Despite efforts to mitigate pollution, Jakarta continues to struggle with poor air quality. The economic impacts of air pollution are substantial, with over 7000 adverse health outcomes in children, 10 000 deaths, and 5000 hospitalizations, resulting in a total annual economic burden of USD 2943.42 million.[20] The most common air quality concern in Jakarta is particulate pollution. PM2.5 concentrations in 2010–2019 consistently exceeded the annual Indonesian ambient air quality standard (NAAQS) of 15 μg m^{-3}.[17]

Particulate source apportionment, therefore, is an essential tool in a strategy to control emission sources.[21] Previous studies in Jakarta were primarily based on measurements at a single site representing the traffic source[15] and city centre[16,17] in Central Jakarta. However, due to local or long-distance sources, topography, and meteorological factors, PM2.5 concentrations[22] and composition[23] could vary spatially. The chemical composition of particulates is a key factor influencing their spatial variations. Understanding the composition of particulates and the sources of each chemical element can profoundly impact the effectiveness of air pollution reduction strategies. Therefore, this research, which provides more information on the typical composition and the attribution of sources in various Jakarta areas, could significantly enhance air pollution control action.

This research aims to provide the first comprehensive observation of the spatial variability in the chemical composition of particulates and their potential source attribution at multiple sites along the north–south transect in Jakarta. Each site location represented diverse geographical and urban characteristics, which may reveal specific PM characteristics of the area, and would benefit the local authorities in determining a more targeted air pollution reduction strategy, for improving air quality in Jakarta.

2 Methods

2.1 Sample collection and chemical component analysis

In this study, we evaluated the particulate concentrations at three distinct locations in Jakarta, namely Kelapa Gading in North Jakarta/NJ (6°9′13.309″S, 106°54′39.586″E), Kuningan in Central Jakarta/CJ (6°13′34.420″S, 106°50′5.330″E), and Jagakarsa in South Jakarta/SJ (6°21′24.050″S, 106°48′12.550″E) (see Fig. 1). The site backgrounds at NJ, CJ and SJ were characterized as industrial, road traffic and suburban, respectively.

Our sampling sites were strategically located at or near the Air Quality Monitoring Stations (AQMS) owned by the Jakarta Province Environment Agency. At the NJ and SJ sites, the samplers were positioned on the rooftops of the AQMS containers, approximately 5 m above the ground. At the CJ site, we mounted the sampler on the roof of a fourth-floor building. The Dichotomous Gent stacked filter unit (SFU) samplers, operating at a flow rate of 15–18 L m^{-1}, collected fine (PM2.5) and coarse (PM2.5-10) particulates using 0.4-μm and 8.0-μm Nucleopore® filters, respectively.[24]

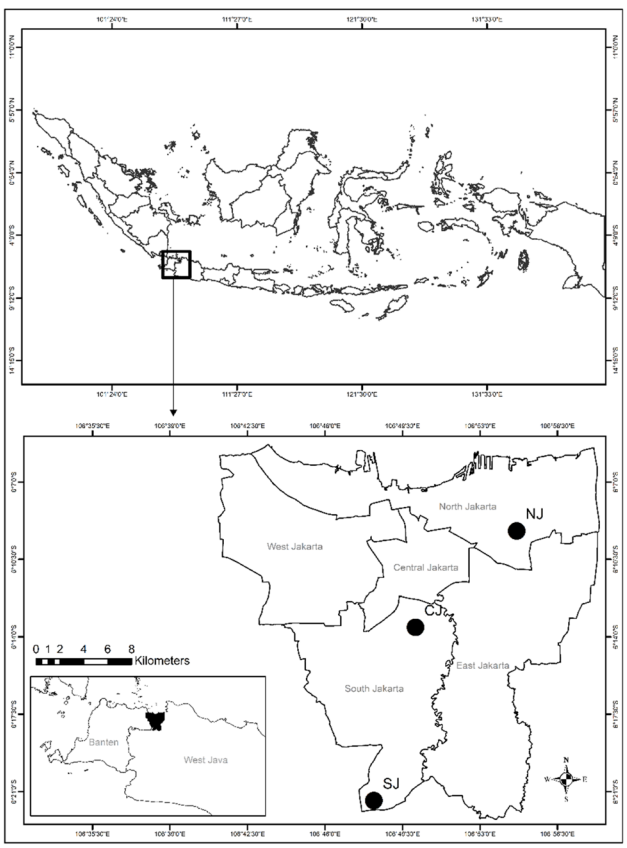

Fig. 1 Sampling locations in NJ (AQMS-Kelapa Gading), CJ (DLH DKI Jakarta), and SJ (AQMS-Kebun Bibit).

Particulate matter concentration is higher during the dry season.[17,18] Therefore, the sampling was conducted during the dry season from June to September 2018, when peak concentrations usually occur. We sampled fine and coarse particulates for 24 hours on alternate days. Sampling was conducted at the three sites on the same days, three to four times a week, primarily on workdays. We collected 32 and 30 samples for CJ and SJ, respectively. However, in NJ, we encountered difficulty in maintaining a similar number of samples due to a non-technical problem regarding access to the AQMS compound. Nevertheless, we only collected 13 samples. Although limited, we considered 13 samples from the driest months to be sufficient to characterize the dry season, as they represented the peak particulate season.

Upon sampling, the samples were stored in sterile plastic Petri dishes and preserved in a controlled environment to ensure mass stabilization. The filters were equilibrated in a controlled environment room where the humidity and the temperature were maintained at (45 ± 5)% and (20 ± 2) °C, respectively. This prevented the effect of moisture on the filters' weight. We weighed the filters after at least 24 hours of stabilization. The particulate matter mass was determined by gravimetric analysis using a highly precise Mettler Semi-Toledo MX5 microbalance with a precision of ±0.001 mg. We obtained the particulate mass by subtracting the weight of the filter before sampling from the weight of the filter after sampling. The mass of the particles is divided by the air volume that passed through the filter to obtain a concentration in μg m^{-3}. We calculated PM10 as the sum of PM2.5 and PM2.5-10.

The EEL model 43D Smoke Stain Reflectometer (Diffusion Systems Ltd) measured the reflectance of black carbon (BC) concentration. This instrument measures the reduction in reflected white light.[24–26] Elemental concentrations were analysed using energy-dispersive X-ray fluorescence (EDXRF) at a nuclear analytical laboratory at BRIN Bandung, Indonesia. The analysis was performed by using an EDXRF Epsilon5 instrument manufactured by PANalytical. The instrument is equipped with an X-ray generator (Sc/W tube, 600 W with a maximum of 24 mA and voltage of 100 kV), using a high-resolution germanium detector, featuring a beryllium window of 150 μm thickness, and a surface area of 30 mm^2. The experimental setup used in the XRF analytical method was described elsewhere.[27,28]

The elements sodium (Na), magnesium (Mg), aluminum (Al), silicon (Si), sulfur (S), potassium (K), calcium (Ca), magnesium (Mg), titanium (Ti), vanadium(v), chromium (Cr), manganese (Mn), iron (Fe), cobalt (Co), nickel (Ni), copper (Cu), zinc (Zn), lead (Pb), arsenic (As), chloride (Cl), and bromine (Br), phosphorus (P), and scandium (Sc) were measured and validated by using standard reference materials with the standard reference material (SRM) National Institute of Science Technology NIST 2783 Air Particulate in Filter Media certificate. The results showed good agreement with certified values, in the range of 92–109%.[27,28] No systematic bias was observed; therefore, correction factors were not applied. The uncertainty was primarily influenced by the counting statistics of the XRF instrument, which were taken into account during data interpretation and factor analysis.

2.2 Data analysis

The data screening process was crucial in ensuring the quality of analysis, which identified values below the detection limit (DL) and missing data (MD). The value of DL/2 was used to replace concentrations below DL, while MD was converted to the geometric mean.[29] Phosphorus (P), Co, Sc, Ag, Ba, Pd, Sn, Te, Sb, and Mg for both coarse and fine particulates at all locations had MDs larger than 50% or below DL data. Vanadium in the fine fraction also had MD values of 84%, 60%, and 90% at NJ, CJ, and SJ, respectively. Therefore, these elements were eliminated from the data set to prevent bias in further analyses. In the next step, the cleaned PM2.5, PM2.5-10 and meteorological data were subjected to statistical analysis, for the total mass of particulates and the chemical elements. We used the open-source statistical analysis of Open-Air RStudio for data analysis.[30]

2.2.1 Statistical analysis. The ratios of PM2.5/PM10, BC/PM2.5, and BC/PM10 were determined by using the regression slope using the Reduced Major Axis (RMA) method to indicate the proportion of fine particles in PM10.[31] We transformed data that did not adhere to standard distribution assumptions before applying the parametric statistics method. The analysis of variance (ANOVA) test, followed by the Tukey–Kramer *post hoc* test, were used to examine the spatial variations of PM concentrations. We used the Pearson correlation to predict the associations between chemical elements to estimate their source contributions to particulates. The correlation measures the strength and direction of association between two variables by examining the linear relationship between them. The correlation (r) between −1 and 1 represents a negative and a positive association. Values of less than 0.4 are categorized as weak, those from 0.4 to less than 0.8 as moderate, and those above 0.8 as strong correlations.[3,32]

The Principal Component Analysis (PCA) with varimax rotation identified the pollutant-source attributions to maximise the variance of the correlation results. The variance represents the component patterns by bringing variable loadings towards values of 0 or 1 on the given component, resulting in a more balanced outcome. Based on eigenvalues greater than or equal to 1, we selected four factors as potential sources of pollution to ensure a comprehensive understanding of the pollution sources. Due to the limited dataset, we processed the NJ dataset using the Single Key Tracers (SKT) approach combined with Multiple Linear Regression (MLR) to mitigate the issue of a singular matrix.[33] This method was applied to identify the most highly correlated representative substance and determine the relative contribution of each selected variable.

2.2.2 Reconstructed mass (RCM). The reconstructed mass (RCM) method is a comprehensive quality assurance tool for the measured particulate mass. It compares the gravimetric mass with the mass estimated from a set of equations. These equations represent major components in the airborne particulate matter samples. It commonly consists of anions, cations, elements including metals, and organic and elemental carbons. The RCM method's key role is to find closure between the

measured particulate matter mass and the sum of the reconstructed mass, thereby accounting for unmeasured species and ensuring the accuracy of the measurement.[34] The equations used for RCM are as follows:

$$\text{RCM} = [\text{sea salt}] + [\text{ammonium sulfate}] + [\text{crustal}] + [\text{biomass burning}] + [\text{black carbon}] + [\text{trace elements oxides}] \quad (1)$$

$$\text{Sea salt} = \text{Cl} + 1.4486\,[\text{Na}] \quad (2)$$

$$\text{Ammonium sulfate} = 4.125\,[\text{S}] \quad (3)$$

$$\text{Crustal} = 3.48\,[\text{Si}] + 1.63\,[\text{Ca}] + 2.42\,[\text{Fe}] + 1.94\,[\text{Ti}] \quad (4)$$

$$\text{Biomass burning} = [\text{K}] - 0.6\,[\text{Fe}] \quad (5)$$

$$\text{Black carbon} = [\text{BC}] \quad (6)$$

$$\text{TEO} = 1.47[\text{V}] + 1.29[\text{Mn}] + 1.27[\text{Ni}] + 1.25[\text{Cu}] + 1.24[\text{Zn}] + 1.08[\text{Pb}] + 3.07[\text{P}] + 1.31[\text{Cr}] \quad (7)$$

Eqn (1) determines the sum of major aerosol chemical components to reconstruct PM2.5, PM2.5-10, and PM10 masses. Based on RCM that considers six pseudo-sources, particulates are identified as coming from sea salt, ammonium sulfate $(NH_4)_2SO_4$), the Earth's crust, biomass burning, and oxides of trace elements.[35–37] Eqn (2)–(7) were used to calculate the contribution of each pseudo source. Eqn (2) represents the marine contribution from sea salt, using the measured amounts of sodium and chloride. A factor of 1.4486 is the mass concentration ratio of all elements to Na concentration in seawater, except that of Cl.[38,39] Eqn (3) represents sulfate contribution, assuming sulfur fully neutralizes ammonium as $(NH_4)_2SO_4$) instead of sodium as $Na_2(SO)_4$. This assumption was made based on Critical Relative Humidity (CRH), a certain humidity threshold that absorbs water vapor from the atmosphere, where the CRH of $(NH_4)_2SO_4$ is lower than that of Na_2SO_4.[40] The multiplicative factor 4.125 in eqn (3) accounts for ammonium ion and oxygen mass.[36,37] Eqn (4) shows soil as a particle source predominantly found in the Earth's crust as Al_2O_3, SiO_2, CaO, and Fe_2O_3 oxides. Black carbon represents elemental carbon or "soot"– containing carbon (C) that has no multiplier (see eqn (6)). Lastly, eqn (7) is for Trace Element Oxide (TEO) that was assumed to be present in the oxide form since its actual form cannot be identified clearly.[37]

2.2.3 Conditional bivariate probability function (CBPF). Several studies have used the Conditional Bivariate Probability Function (CBPF) to effectively investigate the dominant source of pollutants. The CBPF approach uses wind directions and wind speed data. It is an extension model of the Conditional Probability Function (CPF). The CBPF model identifies sources from various wind speeds and directions in polar coordinates at the measured sites to trace the origin of pollution sources. It also assesses the impacts of the local source(s) by using the wind-pollution concentration relationships.[41–44]

We applied the CBPF model to each chemical element using 30-minute average wind speed and direction data obtained from each AQMS for generating wind roses and CBPF calculation. The model, advancing an ordinary CPF coupled with wind speed as the third variable, constructs CBPF plots. This comprehensive approach explains a wide range of source(s) more effectively, as different sources can be associated with different wind speeds. Eqn (8) provides the CBPF equation, defined by, ref. 44 which further enhances the precision of the model.

$$\text{CBPF} = \frac{m_{\Delta\theta,\Delta u|C \geq x}}{n\Delta\theta,\Delta u} \quad (8)$$

where $m_{\Delta\theta}$ is the number of occurrences from wind sector $\Delta\theta$ (set at $\Delta\theta$: 45°) with wind speed interval Δu having a concentration (C) greater than the threshold value. The chosen chemical concentration (C) applies >75th percentile as the threshold criterion. The x notation represented high percentiles. The total number of occurrences from the wind sector is determined by using $n_{\Delta\theta,\ \Delta u}$, where Δu is within a wind direction-speed interval. We excluded calm wind, which was defined as a wind speed less than 1 m s^{-1} from the analysis.

3 Results and discussion

3.1 Spatial variation of fine and coarse particulates

Fig. 2 shows the box plot of PM2.5, PM2.5-10, and PM10 daily concentrations in NJ, CJ, and SJ. The blue and red dashed lines represent the daily thresholds of the National Ambient Air Quality Standards (NAAQS) as outlined in Appendix VII of Governmental Decree No. 22/2021. The values set forth for PM2.5 and PM10 are 55 μg m^{-3} and 75 μg m^{-3}, respectively. The mean PM2.5 concentrations in NJ, CJ, and SJ were 22.74 ± 4.97, 30.99 ± 2.71, and 26.27 ± 3.22 μg m^{-3}, respectively. In the same order, the mean concentrations of PM2.5-10 were 43.71 ± 6.45, 37.23 ± 3.61, and 28.67 ± 3.49 μg m^{-3}.

Tables 1 and 2 summarize PM2.5 (fine) and PM2.5-10 (coarse) masses in micrograms per cubic meter (μg m^{-3}). Black carbon (BC) and elemental concentrations are presented in nanograms per cubic meter (ng m^{-3}). The basic statistical values of PM2.5, PM2.5-10, and PM10 are summarized in Fig. 2. Fig. 2 shows that during the campaign measurements in this study some individual data of PM2.5 and most notably PM10, had violated the NAAQS.

Our study has indicated the potential contribution of local sources of particulate matter. We calculated the PM2.5/PM10 and PM2.5-10/PM10 ratios using data from Tables 1 and 2 to identify the dominant particulate proportion. The PM2.5 concentration data did not indicate a spatial gradation from NJ to SJ. However, the mean ratio of PM2.5 to PM10 increased from north to south. The mean PM2.5/PM10 ratios and 95% CI were 34% (30–38%) for NJ, 45% (43–48%) for CJ, and 47% (43–49%) for SJ. The 95% CI ratios indicated spatial variations in PM2.5 concentrations in the north-to-south direction, with a significant increase in the contribution of PM2.5 to PM10.

Calm wind dominated at all locations, particularly at CJ, where almost 86% of the wind was calm (see Section 3.4). The calm wind and an increase in the PM2.5/PM10 ratio signified local source characteristics and contribution, which at the CJ

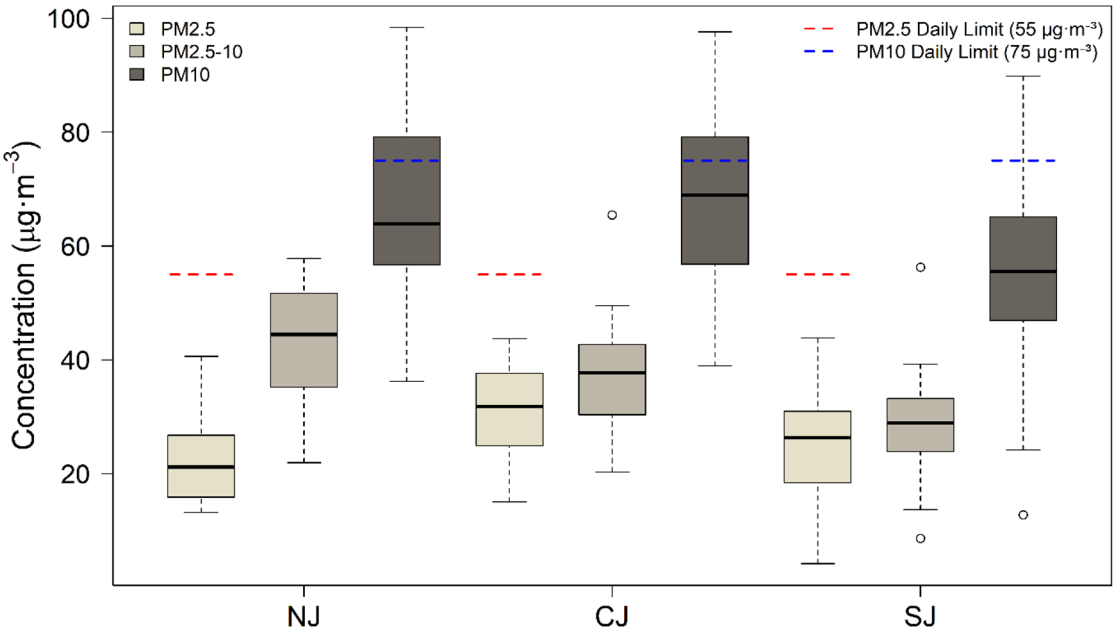

Fig. 2 Boxplot of particulate distribution (PM2.5, PM2.5-10, PM10) in NJ, CJ and SJ.

site could be attributed to nearby vehicular emissions. The wind roses show the significantly high frequencies of calm wind at each location and the stark difference in wind profiles. The prevailing winds from the north, west, east, and south in NJ, SJ, and CJ (see Section 3.4, Fig. 5) and the calm wind proportions confirm that the source strengths at each location play a more significant role in causing differences in concentrations. These findings illustrated the importance of measuring fine and coarse fractions in particulates. The ratios of PM2.5/PM10 could be higher, as the fine particle collection point of Gent SFU is 2.2 microns.[24] More elaboration on specific sources of particulates is provided in Section 3.3.

Contrastingly, the coarse portion in PM10 decreased in the N–S transect. The mean and the 95% CI of PM2.5-10/PM10

Table 1 PM2.5 concentrations (in μg m^{-3}) and elemental concentrations (in ng m^{-3}) in NJ, CJ, and SJ

	NJ			CJ			SJ		
		CI 95%			CI 95%			CI 95%	
Mass	Mean	LL	LU	Mean	LL	LU	Mean	LL	LU
PM2.5[a]	22.74	18.27	27.21	30.99	28.45	33.52	25.17	22.08	28.25
BC	3789.39	3245.17	4333.62	5034.40	4746.97	5321.82	3152.09	2899.76	3404.42
Na	732.68	421.39	1043.97	533.63	439.61	627.65	252.05	205.89	298.22
Al	61.40	42.25	80.56	52.24	41.13	63.34	48.89	38.19	59.58
Si	219.73	185.55	253.91	219.92	200.53	239.32	122.26	105.41	139.11
S	1321.63	1000.51	1642.75	1824.20	1608.12	2040.28	1369.15	1162.11	1576.19
K	272.05	231.64	312.45	351.84	318.02	385.67	260.88	233.86	287.89
Ca	130.55	112.85	148.26	145.24	133.02	157.46	62.01	53.81	70.22
Ti	7.58	6.23	8.93	10.27	9.35	11.19	5.75	4.97	6.53
Cr	1.18	0.75	1.61	1.64	1.39	1.88	1.15	0.95	1.34
Mn	11.05	5.37	16.73	10.55	7.67	13.43	4.89	3.77	6.00
Fe	167.11	137.75	196.47	168.44	153.90	182.99	80.00	69.97	90.02
Ni	1.60	1.33	1.86	1.93	1.68	2.18	1.13	0.94	1.32
Cu	6.71	4.84	8.58	11.35	9.01	13.70	6.33	3.08	9.59
Zn	363.42	143.92	582.91	161.44	122.47	200.41	60.17	48.79	71.55
Pb	38.04	25.06	51.02	28.51	24.03	32.98	18.95	12.64	25.25
As	6.91	4.62	9.19	5.86	4.87	6.85	3.96	3.11	4.82
Cl	21.57	14.09	29.05	21.82	18.67	24.97	15.65	13.99	17.31
Br	14.84	11.26	18.41	14.70	12.81	16.60	9.47	8.58	10.37

[a] Unit concentration in μg m^{-3}.

Table 2 PM2.5-10 concentrations (in μg m^{-3}) and elemental concentrations (in ng m^{-3}) in NJ, CJ, and SJ

	NJ			CJ			SJ		
		CI 95%			CI 95%			CI 95%	
Mass	Mean	LL	LU	Mean	LL	LU	Mean	LL	LU
PM2.5-10[a]	43.710	37.900	49.520	37.230	33.840	40.620	28.490	25.230	31.750
BC	1252.01	1111.50	1392.53	1241.49	1144.70	1338.29	882.22	807.35	957.09
Na	1112.51	822.51	1402.50	676.87	556.99	796.76	560.08	444.69	675.48
Al	901.74	815.80	987.68	844.40	761.39	927.40	628.20	538.70	717.71
Si	1923.49	1730.12	2116.86	1797.63	1624.18	1971.09	1235.35	1077.80	1392.90
S	900.07	751.68	1048.45	867.08	755.74	978.43	657.62	568.99	746.25
K	290.14	257.22	323.06	265.88	240.08	291.68	202.29	181.34	223.24
Ca	1488.58	1330.53	1646.64	1491.50	1349.31	1633.68	933.21	816.65	1049.78
Ti	69.43	62.66	76.21	70.65	63.81	77.49	51.04	44.23	57.86
Cr	3.88	3.19	4.57	5.44	4.69	6.19	2.48	2.23	2.74
Mn	39.53	26.03	53.04	28.11	23.27	32.95	18.79	15.39	22.18
Fe	1154.12	1029.07	1279.17	989.02	891.07	1086.97	646.25	569.18	723.33
Ni	2.42	2.01	2.83	2.34	2.14	2.53	1.72	1.51	1.92
Cu	9.19	7.56	10.82	11.94	10.06	13.82	5.63	4.03	7.22
Zn	812.34	341.86	1282.83	196.34	159.26	233.43	91.08	72.78	109.39
Pb	43.65	24.34	62.96	19.95	16.36	23.55	14.00	9.80	18.20
As	6.68	5.20	8.15	4.89	4.19	5.60	3.25	2.52	3.97
Cl	691.79	509.66	873.93	385.55	286.44	484.66	311.74	236.23	387.25
Br	16.89	9.74	24.03	9.40	7.78	11.01	6.13	5.38	6.87

[a] Unit concentration in μg m^{-3}.

ratios were 66% (62–70) %, 55% (52–57) %, and 53% (51–57) % in NJ, CJ, and SJ, respectively. The significantly high proportion of the PM2.5-10/PM10 ratio near the coast amplified the idea of substantial sea-salt aerosol contribution in NJ. Sodium (Na) significantly contributed to the coarse particles at the NJ site, where crustal elements (Si, Ca, Fe, and Al) also dominated. On the other hand, coarse elemental concentrations were generally the lowest at the SJ site (Table 2). The north–south increasing gradation of BC and elemental mass concentrations in fine particles was apparent from the higher PM2.5/PM10 ratios at the CJ and SJ sites.

Fine particulate (PM2.5) is commonly related to anthropogenic sources.[3,45] These findings illustrated the importance of measuring fine and coarse fractions in particulates. More discussion on specific sources of particulates is provided in Section 3.3. The values of PM2.5/PM10 indicated that more anthropogenic sources contributed to PM2.5 and the total PM10 mass. The highest PM2.5 concentrations at CJ were consistent with the fact that the site is in the most populous area of Jakarta. The influence of urban activity, such as vehicular traffic, explained the increase in PM2.5/PM10 ratios as the sites moved away from the coast.

To examine the spatial significance of fine and coarse particles and each element in their composition, we transformed the data before applying ANOVA and Tukey–Kramer *post hoc* tests to meet normal distribution assumptions. The results (p-value < 0.05) revealed a significantly different means between SJ and CJ (diff = −1.04, p-value < 0.01) and between NJ and CJ sites (diff = −2.54, p-value < 0.01), providing statistical evidence that the PM2.5 mean concentration was indeed the highest in CJ.

The elemental variations reflected the spatial variations of fine and coarse particulates. Black carbon in PM2.5 masses was 3–4 times larger than that in the coarse fractions. The fractions of fine BC in PM10 were 75%, 80%, and 78% in NJ, CJ, and SJ, respectively. The large proportion of BC in fine particles at all sites suggested that its primary source was incomplete combustion, which could originate from traffic congestion, waste, biomass burning, and other fossil fuel combustion.

The second largest fraction of fine particles in PM10 was S, which comprised 59% in NJ and 68% in CJ and SJ, respectively. Like BC, S concentrations increased at the city centre. Data in Table 1 indicated the higher influence of anthropogenic sources on fine particles in CJ and SJ. The Tukey–Kramer *post hoc* test (SI, Table S2) confirmed a spatial variation of PM2.5 concentration, with the mean concentration in CJ being the highest among sites. This result indicates a strong influence of anthropogenic sources in the central urban area, particularly traffic emissions.[46] As CJ has the highest concentration, we found no clear north-to-south descending/ascending PM2.5 concentration pattern. This suggests that local sources, rather than the distance from the coast, are the primary contributors to PM2.5 levels.

In coarse particles, BC and S were not the significant elements. The PM2.5-10 fraction was dominated by Si, Ca, Fe, Al, and K, likely originating from the Earth's crust, as well as Na and Cl from marine sources.[3,47,48] This finding is comparable to that of, ref. 17 which found Na, K, and Cl to be the significant contributors to PM2.5-10. In contrast to PM2.5, the coarse particles showed a decrease in concentration gradient from north to south. This pattern was apparent for Na and the other 14 of the total 18 elements of coarse particles (SI, Table S2).

These elements exhibited the same spatial patterns, indicating that the coarse proportions decreased meaningfully as the sites moved away from the coast (see Table 1a and b). However, other elements, particularly those related to soil dust, did not show any distinct spatial patterns.

Fig. 3 depicts the elemental whisker plots of PM2.5 for all sites. The four highest means of chemical concentrations in PM2.5, in decreasing order of magnitude, were BC > S > Na > Zn in NJ, BC > S > Na > K in CJ, and BC > S > K > Na in SJ. The four elements constituted 27%, 25%, and 19% of the total PM2.5 mass in NJ, CJ, and SJ, respectively.

The precise gradation of Na in PM2.5 and PM2.5-10 from NJ to SJ is a finding with significant implications, likely explaining the diminishing influence of sea spray aerosols on particulate concentrations in the north-to-south transect. The presence of Zn as the fourth element in NJ is an indication of industrial or waste-burning activity. Given the vast industrial estates in NJ, industrial activities are the more likely source. In SJ, the larger K than Na demonstrates that soil dust and biomass burning have replaced sea salt as the third major contributor. A ratio of K/Na larger than 0.036, which is the ratio in the sea water (see Table 4), is a strong indication of non-ssa K from waste burning. The elements with the highest concentrations suggested that anthropogenic sources (represented by BC, S, and K to some extent) overwhelmingly dominate the composition of PM2.5 over natural sources, a finding with implications for pollution control measures. A more detailed discussion on the sources, using Principal Component Analysis (PCA) in Section 3.3, grouped these elements into distinct factors that reflect their respective sources.

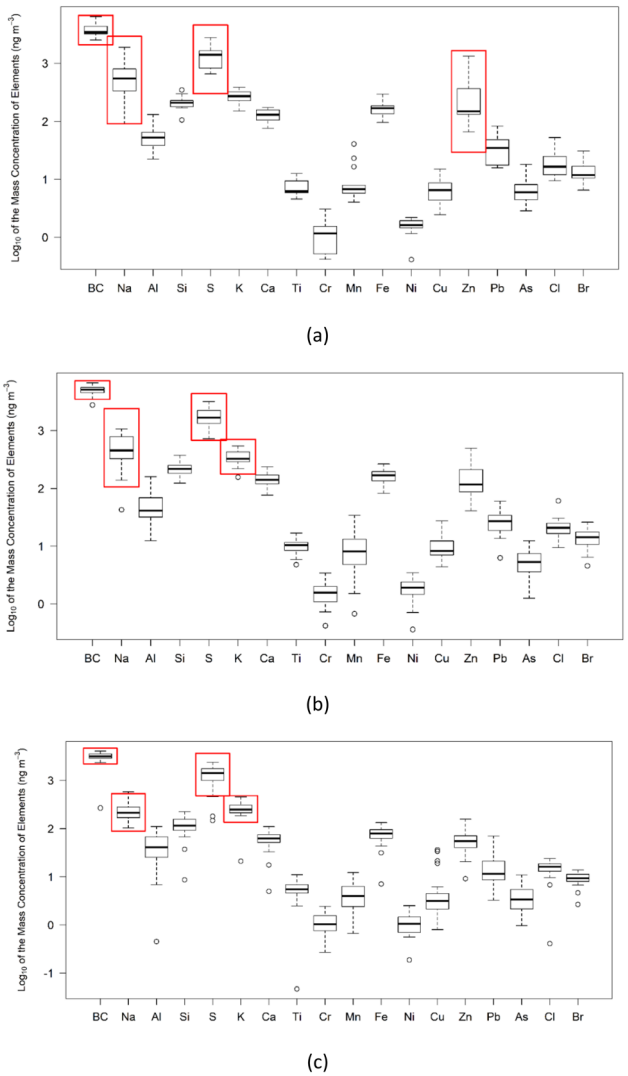

Fig. 3 Boxplot of elemental concentration of PM2.5 in NJ (a), CJ (b) and SJ (c).

In the fine fraction, BC was found to be the highest at all sites. The concentrations and the contributions to the total PM2.5, calculated as the BC/PM2.5 ratio, were as follows: 3.65 $\mu g\ m^{-3} \pm 0.6$ (17%) at NJ, $5.06 \pm 0.31\ \mu g\ m^{-3}$ (16%) at CJ, and $3.15 \pm 0.26\ \mu g\ m^{-3}$ (12%) at SJ. This ratio is a significant indicator of the proportion of BC in the total PM2.5, providing insights into the sources of particulate matter pollution. BC was identified as the primary component at all sites in Jakarta, although it was not the highest in the coarse fraction. This finding is consistent with other studies in Jakarta and other polluted cities, which have found BC to be a significant component of PM2.5.[17,47,48] The BC concentration in PM2.5 was the highest in NJ. Based on the 95% CI of concentration, BC in CJ is in the same order of magnitude. Even in SJ, where the BC contribution of 12% was the lowest, the considerable proportion of BC in total PM2.5 suggests the substantial contribution of incomplete combustion from congested traffic or open burning to fine particle composition.

3.2 Reconstructed mass (RCM)

Fig. 4 exhibits the RCMs for PM2.5 and PM2.5-10, calculated by using eqn (1)–(7). The RCM values represent the percentage of PM2.5 mass attributed to each pseudo-source. In this study, RCM assumes six pseudo-sources at all sites. The average RCM for PM2.5 in NJ, CJ, and SJ is 54%, 49%, and 40%, respectively. The correlation, with a value greater than 0.6 (p-value < 0.01), is a strong indication of well-reconstructed masses.[49] The average mass of PM2.5 consisted of (12–16) % black carbon, (21–24) % sulphate, (3–5) % soil/crustal, (1–4) % sea salt, 1% smoke, and (1–2) % trace elements (Fig. 4a). The remaining mass of (46–60) % was mainly nitrate and organic matter, which were not measured in this study.

Another study reported that organic matter and nitrate accounted for $28 \pm 11\%$ and 5–15% of the mass, respectively.[50] The RCM of PM2.5-10 (Fig. 5b) shows a relatively similar percentage of ammonium sulphate of (20–24) %, but completely the opposite for other sources. Smoke was only significant in SJ with a much larger value of 7.1%. Sea-salt (3.6–8.8%), TEO (0.7–4.3%), and mostly crustal proportions were significantly larger (20–35%). Contrastingly, the BC percentage of 2.4–9.8% was smaller than that in fine particles. The RCM results indicate that secondary particles and soot from incomplete combustion were the primary contributors to fine particles, while soil dust contributed significantly to coarse particles.

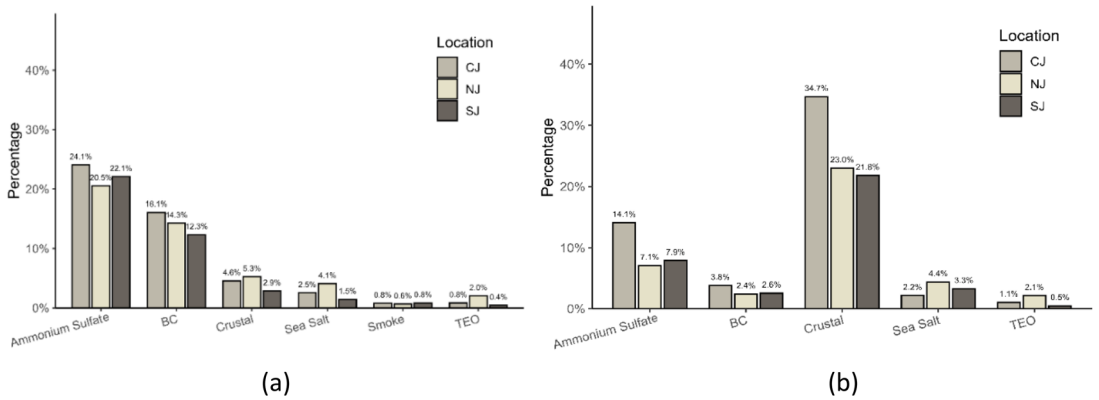

Fig. 4 Reconstructed mass of (a) PM2.5 and (b) PM2.5-10 for all three sites.

Our study, while comprehensive, also has certain limitations. For instance, the conversion of organic components was not conducted due to the XRF technique's inability to measure O and H components related to OC. In addition, inorganic ions such as nitrate (NO_3^-) and ammonium (NH_4^+), and water vapor were not calculated because they readily volatilized from the filter during sampling and measurement.[34] However, due to methodological limitations, particularly the absence of organic carbon (OC), elemental carbon (EC, separate from BC), and inorganic compound measurements (such as nitrate, sulphate, ammonium, *etc.*), a complete mass closure could not be achieved. Despite these limitations, this analysis has provided valuable information on possible sources of the elements in fine and coarse particulates in Jakarta.

3.3 The particulate mass source identification

PM2.5, a significant threat to public health, is a key focus in air quality management.[21] Coarse particles, though important, can be trapped in the upper respiratory tract. However, fine particles, with their ability to penetrate deep into the lungs and enter the bloodstream, pose a higher risk of heart attacks, strokes, and premature death.[51]

The urban areas, as we discuss fine and coarse particulates, are more likely to be affected by PM2.5 from anthropogenic sources.[52,53] We present the PM2.5 source attribution using PCA and CBPF and provide the results for coarse particulates in the SI. PCA was applied to the CJ and SJ sites, and SKT-MLR to examine source attribution in NJ, due to the limited number of data points at this site. These findings are of utmost importance in understanding and addressing the health impacts of PM2.5.

PCA indicated four PM2.5 and PM2.5-10 pollutant sources at CJ and SJ. The cumulative variances obtained for fine and coarse particles were 76.3% and 83.5%; and 76.7% and 86.1% in SJ, respectively. Loading factors represent the correlation between factor scores and the original variables.[33] Selected marker elements based on loading factor values > 0.5 are indicated in bold in Table 3 for PM2.5 and in SI, Table S4 for PM2.5-10.

In the fine fraction of CJ and SJ, the PCA's Factor 1 comprised Al, Si, Ca, Ti, and Fe, which corresponded to crustal elements. At the CJ site, BC was a prominent feature in Factor 1, indicating fuel combustion products associated with congested traffic. The appearance of BC suggests that CJ's Factor 1 primarily represents road emissions, a mixture of soil, road dust, and tailpipe particle emissions.

The coarse fraction of the particulates is also strongly attributed to road emissions, with BC and all crustal elements having high loading factors in Factor 1. In both CJ and SJ, Br appeared in Factor 1 with a modest loading (0.53–0.57). Lead and arsenic were additional coarse elements found in CJ, likely

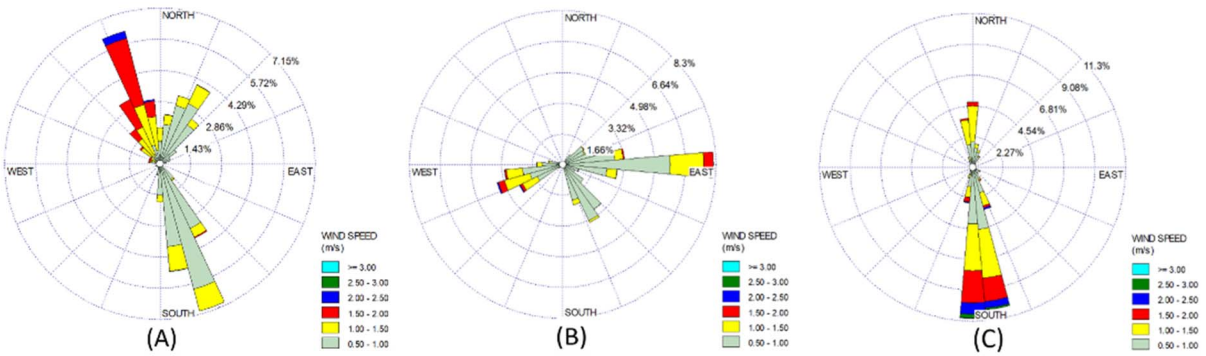

Fig. 5 Wind rose during the sampling period in three sites in NJ (A), CJ (B) and SJ (C).

Table 3 Principal component analysis (PCA) varimax rotation factor loadings of fine particles for CJ and SJ

	Central Jakarta (CJ) site				South Jakarta (SJ) site			
Elements	Factor 1 road emission	Factor 2 Indus- trial/ coal burning	Factor 3 refuse/ biomass burning, sea salt	Factor 4 vehicle fuel	Factor 1 road dust	Factor 2 Indus- trial/ coal burning	Factor 3 refuse/ biomass burning	Factor 4 vehicle fuel
BC	**0.548**	0.383	0.303	0.324	0.221	0.168	**0.899**	0.258
Na		0.474	**0.673**		0.235	0.308		0.433
Al	**0.701**		0.138		**0.767**		0.378	
Si	**0.919**		0.168	0.162	**0.894**		0.342	0.204
S	0.283	0.338	0.148	**0.668**	0.553	0.235	—	**0.668**
K	0.262	0.238	**0.807**		**0.670**		**0.637**	0.220
Ca	**0.935**		0.125	0.106	**0.901**		0.129	0.188
Ti	**0.846**	0.228		0.237	**0.844**	0.117	0.378	0.157
Cr	0.294	0.452		**0.532**	0.363	0.261	0.294	0.450
Mn	0.345	0.245	0.444	0.268	0.424	—	**0.605**	
Fe	**0.786**	0.312	0.269	0.375	**0.760**	0.187	0.428	0.404
Ni				**0.842**				**0.743**
Zn	0.186	**0.723**	**0.506**		0.157	**0.738**		0.484
Pb	0.164	**0.885**	0.206			**0.921**	0.11	
As		**0.901**	0.216	0.155		**0.953**	0.105	
Cl	0.374	0.234	**0.702**		0.406	0.216	**0.518**	0.126
Br			**0.845**	0.329	0.481		0.174	**0.630**
SS loading	4.430	3.240	3.114	2.189	5.135	2.719	2.615	2.563
% variance	26.1	19.1	18.3	12.9	30.2	16	15.4	15.1
% cumulative variance	26.1	45.1	63.4	**76.3**	30.2	46.2	61.6	**76.7**

Table 4 Identification of non-SSA particulates by using the ratio of Na/Cl and K/Na

		Na/Cl		Na/Cl ratio to sea–water		K/Na		K/Na ratio to sea-water	
		Fine	Coarse	Fine	Coarse	Fine	Coarse	Fine	Coarse
NJ	Mean	36.89	1.73	67.07	3.14	0.80	0.31	22.12	8.64
	Median	36.91	1.76	67.11	3.21	0.44	0.29	12.28	8.08
	LL95%CI	25.40	1.43	46.17	2.60	0.18	0.23	22.50	6.35
	UL95%CI	48.38	2.02	87.96	3.68	1.41	0.39	45.02	10.93
CJ	Mean	25.20	2.24	45.82	4.08	0.94	0.49	26.15	13.67
	Median	22.40	1.81	40.73	3.28	0.80	0.45	22.35	12.52
	LL95%CI	19.47	1.69	35.40	3.07	1.07	0.40	29.88	11.18
	UL95%CI	27.40	2.80	49.81	5.08	1.44	0.58	39.70	16.15
SJ	Mean	15.98	2.25	29.06	4.10	1.25	0.68	34.79	18.98
	Median	14.04	1.97	25.53	3.58	1.32	0.40	36.53	11.21
	LL95%CI	13.09	1.72	23.80	3.13	1.07	0.30	29.88	8.25
	UL95%CI	18.88	2.79	34.33	5.07	1.44	1.07	39.70	29.72

related to emissions from industrial sources in the west direction during high-speed wind (>2 m s^{-1}) events, as shown by CBPF profiles (SI, Fig. 2b). This underlines the significant role of high-speed wind in the dispersion of industrial emissions and its impact on air quality in the area, although wind speeds greater than 2 m s^{-1} in CJ were only acquired in less than 15%.

The high concentration of BC in fine particles in the city centre (CJ) was likely due to fuel combustion in diesel and gasoline engines. Conventional diesel engine technology (DET) can produce 33–90% BC, as older engine technology tended to emit more pollutants. The later DET with improved technology emitted 50% less.[54] Gasoline engines' exhaust gas contained approximately (25–42) % BC. DET could emit particulates and BC per km, up to 25–300 times greater than that of gasoline engines.[55]

In Indonesia, the first regulation stipulated EURO II engine technology for all types of motor vehicles in 2005. In 2015, there was an improvement in motorcycle engines to EURO III. Subsequently, for passenger cars, EURO IV became the standard in 2017.[56] In gasoline cars, the EURO IV regulation took effect immediately in 2018. However, due to the longer time needed to provide the diesel fuel required for EURO IV, the regulation for

diesel cars was only implemented in 2022. Thus, until now, motorcycles use EURO III engines, and in 2018, all diesel vehicle engines were still EURO II.

With the heaviest traffic in CJ, the city centre shows the highest concentration of BC in both fine and coarse particles. Factor 1 of the coarse fraction further supports this, with S

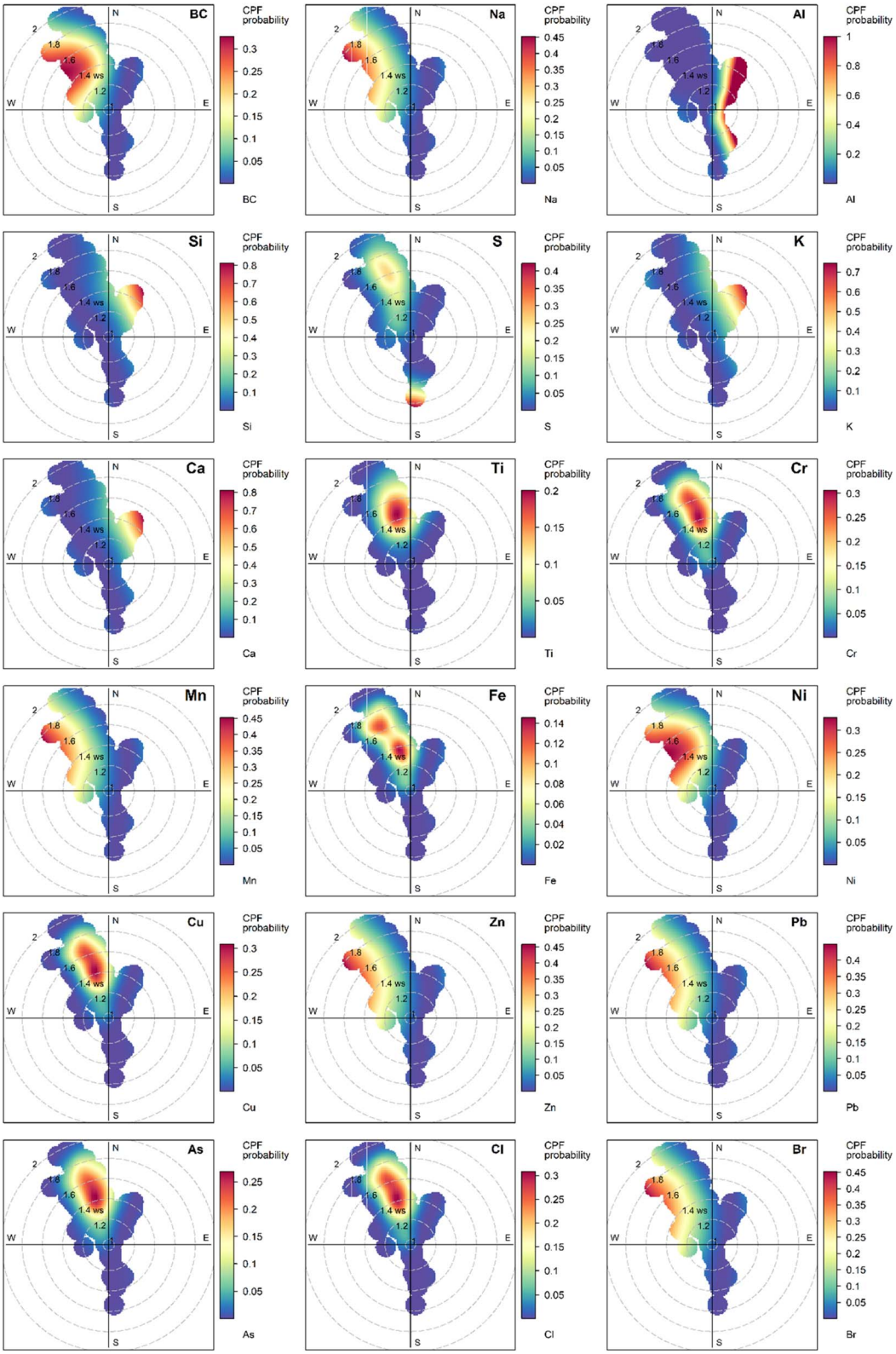

Fig. 6 CBPF of fine particle elemental composition at the NJ site.

(loading = 0.910) appearing alongside BC (loading = 0.898) and other road emission-related elements (SI, Table S4). These results provide strong evidence that traffic is indeed the primary source of fine and coarse particles in the city centre, highlighting the significant impact of human activities on air quality.

While BC is not a significant factor in Factor 1 of fine particles in SJ, road dust is a common factor in both CJ and SJ. In SJ, soil-origin elements in Factor 1, which correlate with K, suggest that soil dust is the primary source. However, like in CJ, there were loadings of BC and S in the PM2.5-10 fractions of Factor 1, indicating a mixture of road dust in coarse particulates. The PCA results for the fine particles at the CJ and SJ sites accounted for 26.1% and 30.2% of the variance, respectively. For coarse particles, the percentage variances were 47.6% in CJ and 50.1% in SJ, making them the most significant contributors to the associated cumulative variances.

Factor 2 of PM2.5 in CJ (19.1%) and SJ (16%) was found to be primarily composed of Zn, As, and Pb. The CBPF results (see Section 3.5) indicate a high likelihood of fine particles Zn, As, and Pb being carried by westward winds at CJ and SJ (Fig. 7 and 8). The PCAs and CBPFs of coarse particles closely mirrored those of fine particles (SI, Table S4, Fig. S2 and S3), reinforcing our findings. These results strongly suggest that industries, including those involved in coal combustion,[57,58] are the predominant sources of these particles.

The alignment of Zn, As, and Pb in both fine and coarse particle sources, with the dominant westerly wind direction, suggests industrial sources as the primary contributors. Although PCA is not available for NJ, the similarity of fine and coarse CBPF profiles of Zn, Pb, and As in NJ (fine particles in Fig. 6 and coarse particles in SI Fig. S1) further enhances the conclusion of industries in the Tangerang area as the sources of fine and coarse particles of Zn, Pb, and As at all sites.

The inference that Pb and As primarily originate from coal combustion is not just a mere observation, but a significant finding. This observation is underscored by the remarkably high factor loadings of Pb and As, at 0.90 or higher, in the fine fractions of CJ and SJ, as well as in the coarse fraction of SJ. Even in the coarse fraction in CJ, where Pb and As are mixed with BC, S, and all crustal elements in Factor 1, their lower factor loadings compared to Factor 2 still points to their association with coal combustion. The CBPFs of these elements, which showed high probability from the west (industrial regions in Tangerang), further solidify this conclusion. This result provides an unambiguous understanding of coal combustion as the primary source of Pb and As, underlining the importance of our research in identifying pollution sources.

Zinc was consistently found in the same factor with Pb and As (Factor 2) in PCA of CJ and SJ, both in the fine and coarse fractions. In addition, in the fine fraction of CJ, Zn also appeared in Factor 3, suggesting that refuse burning[59,60] was the source. Zinc had a lower factor loading compared to As and Pb in Factor 2, and in Factor 3, compared to other elements. Zn is associated with various industries,[16,33,50] incineration activities,[59] refuse burning, tailing oil[60] and vehicle emissions.[59,61] It appears that in the fine fraction, Zn originated not only from a single type of industrial source but also from other sources, such as waste burning. In an industrial source, the appearance of Zn could come from two possibilities. Firstly, it is from coal containing Zn. Secondly, which applies to both coarse and fine particles, Zn originates from industrial entities that used coal as their energy source, causing the elements to be released simultaneously from the same area or direction.

Factor 3 of PM2.5 in CJ correlated with K, Br, and Cl, with loading factors of 0.807, 0.845, and 0.702. Sodium and Zn also appeared, but with lower loading factors. The appearance of Zn in Factor 3 with K, which has a high factor loading, supports the argument of waste burning as the source of Zn. These elements accounted for 18.3% of the variance. Apart from sea salt, fuel oil and industrial and combustion processes emit Na,[62] Br[63] and Zn. Br can be released from waste burning,[64] vehicle fuel combustion,[65] and industrial sources.[63] All these activities can also release bromine chloride (BrCl) gases, producing fine bromide aerosols. Bromide correlation loading in Factor 3 with K and Zn as well as Na and Cl in CJ could represent both natural and anthropogenic nss-Na, likely from waste/refuse burning.[4,64,66] In CJ, Br seemed to originate from multiple sources. Considering the land use type in CJ, fuel combustion and waste burning are more likely anthropogenic sources, although it did not rule out natural sources.

Sodium, chloride, and potassium are commonly known to have a marine origin. We calculated the mass ratio of Cl and K to Na to examine the possible contribution of sources other than sea-salt aerosols. The Na/Cl ratio in sea salt is 0.55 (or Cl/Na = 1.81), and that of K/Na is 0.036. Thus, we can estimate the contribution of anthropogenic activities to aerosol Na and K from the ratios of Na/Cl[66] and K/Na,[62] which are higher than their ratios in seawater. The calculation is based on the assumption that all chlorine is of marine origin.[62]

A value of Na/Cl larger than the ss-Na/Cl ratio may indicate two causes. Firstly, excess Na due to chlorine depletion, as air mass travels through a polluted urban area. NaCl reacts with acidic gases in the atmosphere, such as nitric acid (HNO_3) and sulfuric acid (H_2SO_4).[67] These reactions lead to the displacement and volatilization of chloride as HCl gas, leaving behind Na in the particulate phase.[68] Secondly, the presence of Na from anthropogenic and/or other natural sources, which adds to Na concentration.[69]

Table 4 presents the calculated Na/Cl and K/Na ratios. The North Jakarta area, being close to the coast, would typically have abundant fresh sea salt. However, the remarkably high Na/Cl ratios (Table 4) and Na mass concentration (Table 1) in this area strongly suggest Cl depletion and nss-Na input into the fine particles.

The average Na/Cl ratio of the fine particles in NJ is 37, in contrast to 16 in SJ. While decreased, these ratios were approximately 67 to 29 times higher than the ratio in seawater. In the coarse particle fraction, we found a similar trend. Although much lower than that in the fine fraction, the values of Na/Cl in coarse particles ranged from 1.73 to 2.25 (or 3.14 to 4.1 times the seawater ratio), where the average coarse fraction Na/Cl in NJ was the highest. However, instead of decreasing, with the longer distance from the coast, the average ratio in SJ of coarse particles

Table 5 The PM2.5 SKT-MLR results of the NJ site

Source	Soil (Si)	Sea salt (Na)	Traffic (S)	Industry (As)
ng m^{-3}	220 ± 38	733 ± 346	132.2 ± 357	6.9 ± 4.2
%Tracer relative contribution	**14.64%**	**6.72%**	**53.94%**	**24.69%**

was slightly higher than that in CJ. The SJ Na/Cl ratio in the coarse fraction suggests the addition of Na.

The Factor 3 loadings of fine particles in CJ also included K and Zn, in addition to Na, Cl and Br, suggesting a mixture of marine aerosols as a familiar natural source, and anthropogenic sources. In Factor 3 of fine particles in SJ, BC, which typically occurs during low-temperature oxidation, appeared with the highest loading factor of 0.899. BC together with K, as a known marker of biomass burning,[62] appeared in Factor 3 with Mn and Cl. These elements in Factor 3 in SJ indicate municipal waste burning.

The inclusion of K, Mn, and BC in SJ's Factor 3 is a unique and plausible finding, considering the predominant residential land use types at SJ. The ratio of fine K/Na of 1.25 (or almost 35 times the ratio in the sea water) in Table 4 further implicates nss-K[62] of biomass burning as a significant contributor to Factor 3 in SJ. The absence of Na as a significant contributor to the fine fraction of particles in SJ further confirms that sea salt is not a significant contributor to PM2.5 in SJ, a unique characteristic of this location. However, in the coarse fractions of CJ and NJ, only Na, Cl, and Br appeared in Factor 3 with factor loadings of 0.843, 0.783, and 0.503 (see SI Table S4). Factor 3 components suggested that these elements come from the same source. Section 3.5 provides more detailed explanation of this possible nss-natural source.

Factor 4 of PM2.5 components in CJ were S (0.688), Ni (0.842), and Cr (0.532), which accounted for 12.9% of the variance. In the coarse fraction, CJ's Factor 4 contained Cu (0.516), Ni (0.808), and Cr (0.504), which represented 9% of the variance. At the SJ site, Factor 4 of the fine fraction contained S, Ni, and Br, comprising 15.4% of the total PCA loading, while its coarse particles only consisted of Cu, with a loading of 0.917, accounting for 7.7% variance. In SJ, fine Br that appeared in Factor 4 with S and Ni clearly represents vehicle emissions.

The S element in sulphate (SO_4^{2-}), a secondary pollutant produced from the oxidation of sulphur dioxide (SO_2),[70] is a significant contributor to sulphate aerosol. As the vehicle's source fingerprints show for diesel fuel and gasoline, sulphur was the second-highest concentration element found at all sites. The sulphur content in diesel fuel sold within the Jakarta Metropolitan Area is 100–120 ppm, and 500 ppm in other parts of Indonesia, whereas the international standard is 50 ppm. This high sulphur content is directly linked to the elevated sulphur concentrations in PM2.5, raising concerns about air quality. The high sulphur levels likely correlate with the increasing motor vehicles in DKI Jakarta. In 2018, private vehicles comprised 82% of the total registered vehicles, with a number that had doubled from 2008.[14]

The highest factor loading of Ni strongly suggested the marker of traffic with much braking due to congestion, which caused tire and brake wear. Factor 4 of PM2.5 containing S together with Ni and Cr in CJ, as the key metal composition of tire and brake,[71] with Ni and Br in SJ, are clear indicators of motor vehicle emissions, from fuel burning as well as the vehicle operational condition, causing frequent braking in congested traffic.

The combined PCA with the CBPF results of sulphur during strong wind (>1.5 m s^{-1}) in Fig. 8 reveal that S, which is mainly emitted from the exhaust tailpipe, could be transported from traffic activity in Central Jakarta. This finding underscores the crucial role of wind patterns in pollutant transport. The CBPF profile indicated that S and, occasionally, Br in the events of high wind speed, have the highest probability of coming from the city centre direction to SJ. In contrast, nickel CBPFs for both fine and coarse particles in CJ and SJ showed a high probability of diffuse and centralized patterns with low wind speeds, suggesting a more localized source. These CBPF patterns strongly supported the argument of road emissions from tire and brake wear. The highest mean Ni concentration of fine particles was also found in CJ, an area known for its congested traffic.

The NJ site, which employed the SKT-MLR approach, exhibited general sources like those observed at CJ and SJ (Table 5). The PM2.5 selected markers, along with their relative contributions, were Si for soil, Na for sea salt, S for traffic, and As for industry and coal burning. Sulphur, representing traffic, emerged as the most significant contributor (53.94%), followed by industrial sources, which accounted for 24.69% of the total. The overall contribution of traffic and industrial sources, at 78.63%, reiterates the argument of Cl depletion due to the oxidation of N and S oxides, based on the Na/Cl ratio in Table 4. The sum of traffic and industrial sources, along with 14.64% soil and 6.72% sea salt, makes up the total contribution of 99%, providing a comprehensive picture of the North Jakarta area. This area, serving as a hub for industries, is a built-up area with toll and main roads accessed by heavy-duty vehicles heading to and from the port. Here, vehicles transporting goods, vessels, and ships using diesel, heavy fuel oil (HFO), and marine diesel oil (MDO) fuels were the primary sources of S emissions. The myriad sources underscore the complexity of the particulate sources in NJ.

NJ area activities are predominantly industrial and commercial, with high traffic of heavy-duty vehicles leading to the port. Most activities in NJ are potential significant contributors of oxidized N and S. Although there is no PCA in NJ, the industrial land use characteristics and the exceptionally high Na/Cl ratio in Table 4 may indicate anthropogenic nss-Na emission influence, and ss-Cl depletion in the respective area. The CBPF profiles of these elements (Fig. 6) backed up this analysis.

3.4 The effect of meteorological factors on the spatial variation of PM concentration

In situ meteorological measurements provided wind speeds and directions at the NJ and SJ sites. In CJ, meteorological data were obtained from the closest measurements at the government AQMS, located approximately 3 km away from the CJ site. Most wind speeds at all sites were categorized as calm (less than 1 m s^{-1}), with data ranging between 0.01 and 1.96 m s^{-1}, 0.01 and 2.20 m s^{-1}, and 0.01 and 3.21 m s^{-1} in CJ, CJ, and SJ, respectively. The proportion of calm wind less than 0.5 m s^{-1} ranged between 44.5–51.40%, while wind speed of 0.5–1.0 m s^{-1} ranged between 26.80% in SJ and 34.4% in CJ, making the total calm wind in NJ, CJ and SJ of 76.10%, 85.80%, and 71.30%. Overall, the average wind speeds were 0.61, 0.45, and 0.7 m s^{-1} at the NJ, CJ, and SJ sites, respectively, indicating that the wind was commonly calm.

We then divided wind data into two groups based on wind speed categories: weak (<1 m s^{-1}) and strong (>1 m s^{-1}) winds. The difference between strong and weak wind was analysed using the Wilcoxon signed-rank test. The concentrations between strong and weak winds were not statistically different at the NJ and CJ sites, whereas they were significant at the SJ site (p-value < 0.05). The wind data support the rose plots in Fig. 5.

The strongest wind in NJ mostly came from north-north westerly (NNW) direction, indicating the influence of land-sea winds (Fig. 5a). In contrast, in SJ, the southern direction acquired the most significant wind direction proportion as well as the strongest wind speeds (Fig. 5c). At all sites, the calm wind dominated, suggesting that the local sources might have contributed more to the particulate concentrations and composition than sources at long-distance locations.

The wind direction pattern at SJ (Fig. 4c) suggests the influence of hill-to-plain/valley winds at this site. The mountain wind may originate from the higher-elevation terrain of mountainous Bogor City in southern Jakarta. In contrast, although it was predominantly calm, smaller proportions of the higher wind speed events in CJ tended to come from easterly and westerly directions (Fig. 4b). The CJ's east-west winds were the typical wind directions in the lower layer of the atmosphere in Indonesia, based on radiosonde data analysis.[11,12] The wind profile underscores the implications of these wind direction patterns for air pollution control strategies, particularly in areas with similar geographical features.

3.5 Conditional bivariate probability function

By removing the influence of calm wind, the CBPF can discern the prevailing winds at each location and pinpoint the potential source locations of PM and each of its elements. Notably, we observed detailed variations in wind speeds, with strong winds within the 1–1.5 m s^{-1} range being less than 20% in NJ and SJ, and only 5% in CJ, making each site's observation unique. Higher wind speeds between 2–2.5 m s^{-1} were a mere 0.2%, 0.1%, and 1.8% at the NJ, CJ, and SJ sites. Only in SJ did we observe strong winds with speeds exceeding 2.5 m s^{-1}, accounting for 0.5%.

3.5.1 Source direction at the NJ site. The NJ's PM2.5 CBPF plots, shown in Fig. 6, clearly demonstrate the strong influence of the northwestern to northern wind quadrant. BC correlated strongly with S (r > 0.8 at the 0.01 level) (SI S1), and both have a similar CBPF from a north-northwest (NNW) direction. BC also showed a higher probability from the west directions with higher wind speed, which might be related to more distant sources of heavy traffic on highways, connected to Tangerang City and the Soekarno-Hatta International Airport.

The CBPFs of Ni, Pb, Zn, Mn, and Br were nearly identical to those of BC, and are indicative of specific industrial sources,[33,59] likely due to the presence of approximately 493 industries in industrial estates in Tangerang and North Jakarta, including galvanized and steelworks.[13,14] In contrast, the CBPF of S with the heavy metals Cr, Fe, Fe, Cu, As, Cl, and As leaned toward the NNW–N direction and resembled that of Na, suggesting sources at the coastal areas. The CBPFs pointed more to the north direction of where the Tanjung Priok Port is located, where the utilisations of HFO, MFO and diesel fuel are more concentrated. The direction of S and As also suggests coal combustion sources. Ti, Cr, Cu, As, and Cl exhibited identical patterns with wind speeds ranging from 1.2 to 2 m s^{-1}, suggesting that the emission sources could be local or originate from industrial sources in North Jakarta. Other PM2.5 elements in NJ showed moderate to low correlations in different directions and strengths. The crustal elements of Si, K, and Ca generally had low probabilities, with a small proportion of high probability toward the northeast.

The CBPFs of BC and S for coarse particles, showing a direction from the north, were more apparent (SI, Fig. S1). The high probability of BC and S that aligns with Al, Si, K, Ca, Ti, Mn, Fe, and Cu elements suggests some common source directions. The similarity of the CBPF profiles could be due to the influence of industrial activities, ship and port emissions, and other crustal element sources on the north coast of Jakarta, particularly from the Tanjung Priok Port.

3.5.2 Source direction at the CJ site. Fig. 7 illustrates the complex wind patterns in CJ, with calm winds 85% of the time and a low probability of west-east winds. These wind directions represent the typical wind pattern in Jakarta. The CBPFs in CJ consistently show a maximum wind speed of only around 1.6 m s^{-1} or less. The densely populated areas in the east and west directions, particularly in Bekasi Regency and Cilegon in Banten, are closely linked to busy roads and industrial complexes.

The CBPFs aligned with the PCA results, indicating that local sources of elements from road dust, vehicle fuel combustion, tire-and-brake wear products, and refuse burning were the primary sources (detailed discussion in Section 3.3). The CBPF plots of fine (Fig. 7) and coarse (SI S2) particles of S, Br, and Cu in CJ were similar at wind speeds lower than 1.2 m s^{-1}, indicating the dominance of local sources of these particle elements. This clear and consistent pattern in both fine and coarse particles, with Pb and Zn, and As in the fine particles showing the highest concentrations like that at the NJ site, introduces assurance in industries in the Tangerang area as the

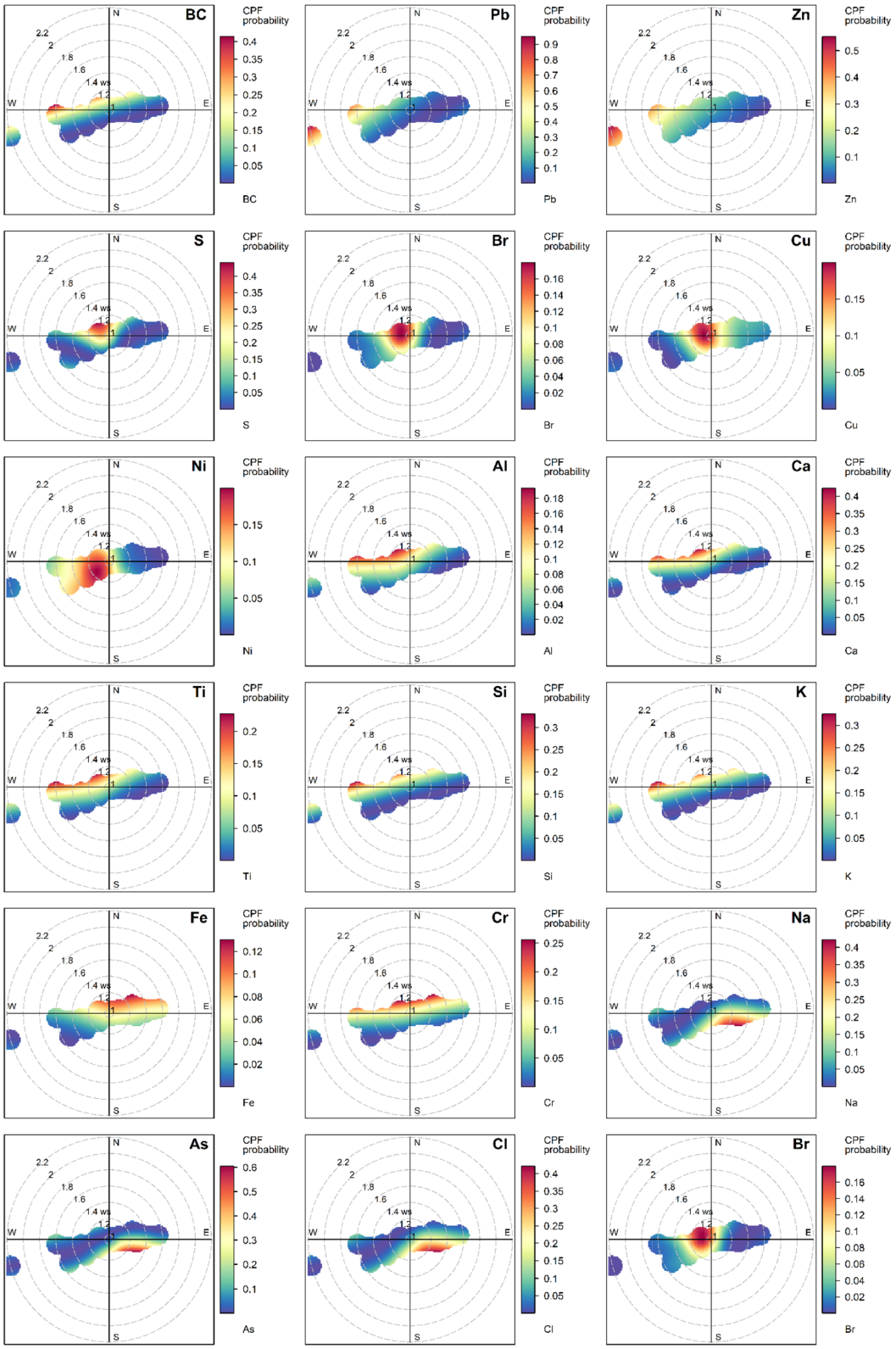

Fig. 7 CBPF of fine particle elemental composition at the CJ site.

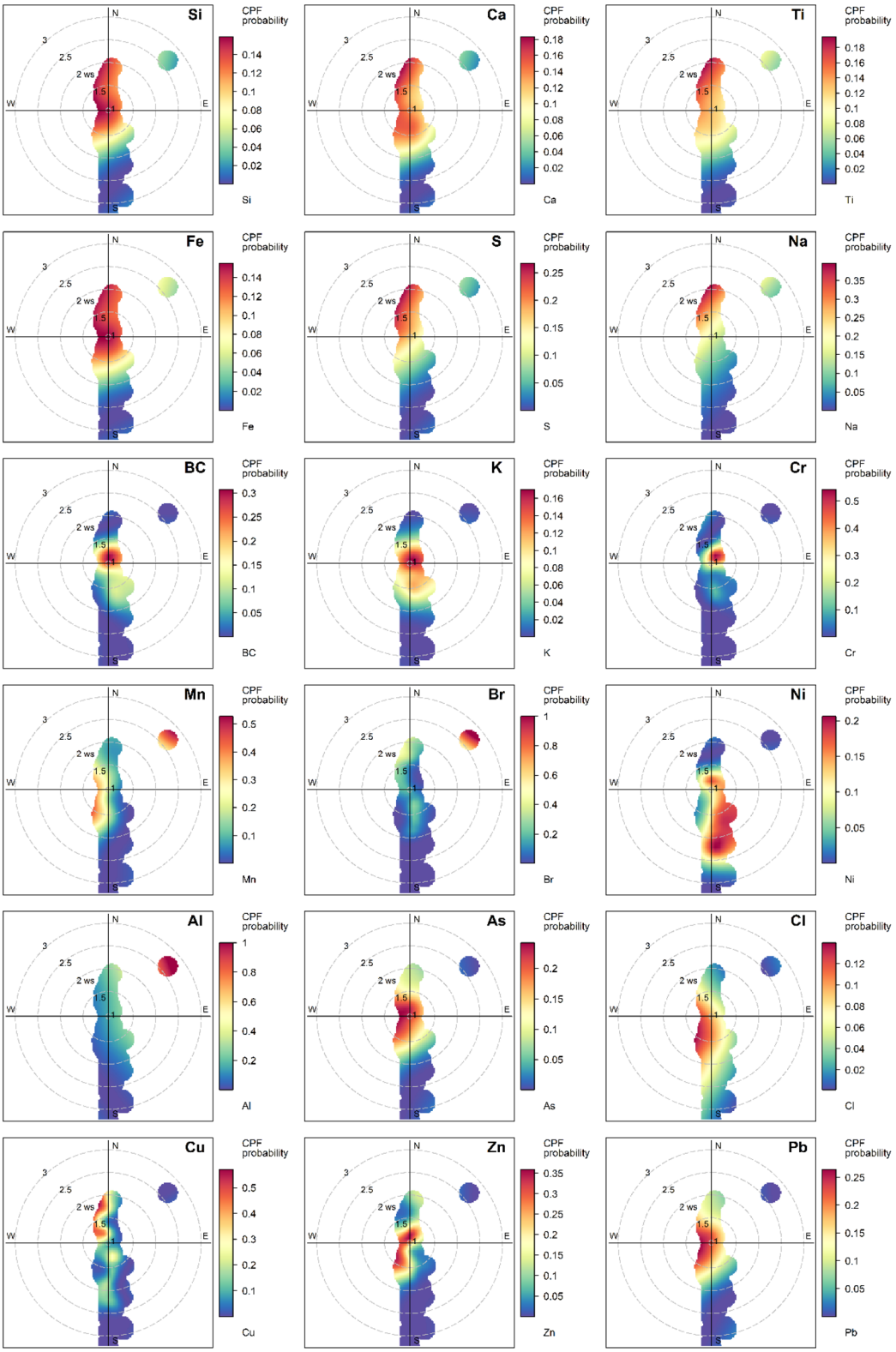

Fig. 8 CBPF of fine particle elemental composition at the SJ site.

sources. The strength probability of Ni in PM2.5 toward the western direction of 1.2–1.8 m s^{-1} matched the location of the nickel smelter and steelworks about 40 km west of CJ. However, Ni in the coarse particles showed a lower probability in different directions from the south.

With smaller probabilities, the CBPFs of Fe and Cr in CJ might indicate the sources in the western and eastern directions. The possible sources of these elements could be the industrial activities of steelworks and metallurgy,[59,72] approximately 30 km east of Bekasi city, as well as industries in the Tangerang area. Relatively high probabilities of BC, Si, K, Ca, Ti, and, to some extent, Al, Cr, and Fe came from the NW, N, and NE directions. However, the wind speeds were considerably low (1.0–1.6 m s^{-1}). In general, the high proportion of calm wind (almost 86%) has corroborated that local activities, including but not limited to vehicular emissions and construction works, were the primary sources of fine and coarse particles in Central Jakarta. A combination of various factors, such as the density of road networks, the large proportion of calm wind, and the spatial diffusion of emissions, adds a layer of complexity to source identification in CJ, making it challenging to determine the source direction precisely.[73] However, the high frequency of calm wind likely plays the most important role in retaining fine and coarse particles either from local or long-distance sources.

3.5.3 Source direction at the SJ site. The relatively dense population in SJ, a leafy area in Jakarta with few industrial activities, has led to some novel findings. All PM2.5 CBPF plots in SJ (Fig. 8) and PM2.5-10 (SI, Fig. S3) showed sources in the north and south directions. The PM2.5 CBPF profiles of Si, Ca, Ti, Fe, S, and, to some extent, Na and Mn were almost identical, showing the highest probability with a relatively high wind speed of more than 2 m s^{-1} from the north direction.

The fine particle CBPF patterns of road emission fingerprints indicated that during relatively higher wind speed, in addition to local sources, S and soil dust could be transported from Central Jakarta to the South. However, the concentrations of typical vehicle source fingerprints were relatively low. Stronger correlations were observed between Si, Ca, Ti, and Fe and crustal elements, such as Al and Si, but lower Na levels indicated a greater contribution from road emissions and soil dust, with less influence from sea salt.

The PM2.5 CBPFs of BC, K, Mn, and Cr were relatively similar, with a high probability of lower wind speeds of around 1–1.5 m s^{-1}. Zn, As, Pb, and Cl were similar, but spreading more from north and south directions. The CBPFs indicated that the sources tended to be local. The CBPFs aligned with the PCA results, which found that BC, K, Mn, and Cl correlated with Factor 3, representing local refuse and biomass burning. This thorough alignment of the CBPFs with the PCA results provides confidence in the accuracy of our findings. The evidence of BC, K, and Mn correlating more with biomass burning in PCA's Factor 3 and S correlated with Br and Ni in Factor 4. This argument suggested that traffic in SJ is heavy but not congested. Sulphur and Br were likely emitted from fuel combustion, and Ni from tire and brake materials.

Sodium in the fine fraction seemed to come from the northerly direction. Interestingly, Na, Cl, and Br in the coarse fraction showed completely different CBPFs, with the highest probability (100%) coming from the south during a high wind speed of over 3 m s^{-1} (SI Fig. S3). Sodium, chlorine, and bromine are typical markers in sea salt. However, the incoming direction was the opposite of the coast, suggesting other sources. Mount Salak is an active volcano[74] in Bogor Regency, approximately 70 km south of the SJ site. Its volcanic fumaroles, such as those from the Kawah Ratu craters, are the probable source of Na,[75] Cl,[76,77] and Br[78,79] aerosols.

To confirm the CBPF results, we run an open-source NOAA HYSPLIT ash plume dispersion model,[80] for the day when wind speeds were the highest (see SI, Fig. S4). The ash dispersion profile demonstrated encouraging support for our findings. The model shows the plume from Mount Salak extending to South Jakarta and bending towards the western area of Central Jakarta. The plume did not extend to the NJ site, which is in the eastern part of North Jakarta. This volcanic dispersion pattern also explains the source for coarse Na, Cl and Br that appeared together in the PCA's Factor 3 (SI, Tabel S4), not only in SJ but possibly also in CJ. The Tukey–Kramer *post hoc* test of coarse Br (SI, Tabel S2) shows that Br concentration in SJ was significantly higher than that in CJ ($p = 0.000$) and in NJ ($p = 0.003$). The coarse Na and Cl were significantly the highest in NJ ($p = 0.000$), but the difference between SJ and CJ of these elements was not significant. This is a plausible indication of volcanic emissions from the south direction becoming additional coarse particle sources of Na, Cl, and Br in SJ, and possibly some smaller proportion of Na and Cl in CJ. Contrastingly, in the fine fractions, the Tukey–Kramer test confirmed a clear north-to-south decrease in Na concentration, where NJ was the highest, followed by CJ and SJ. However, fine Br in SJ was significantly lower than that in CJ and NJ, while there was no difference between Br in NJ and CJ.

4 Conclusions

Our comprehensive study, conducted across multiple sites, has unveiled significant spatial disparities in the concentration of fine and coarse particulates along Jakarta's north–south transect. This finding, coupled with the identification of distinct primary sources at each location, marks our significant understanding of particulate pollution as a complex environmental issue. The PCA, in conjunction with the CBPF that integrates wind speed into the probability function, provides a robust framework for pinpointing source contributions in a monitoring location. This combined method is highly effective for data analysis of our campaign measurements that cannot provide a large amount of data. The method has been rigorously tested and proven robust in detailing local emission influences and estimating the potential contribution of diverse sources from more distant locations, providing reassurance and confidence in our approach.

Although calm wind prevails, the higher wind speeds in Central Jakarta (CJ) resemble the typical east-west winds in Jakarta and other Indonesian regions. In North Jakarta (NJ), the higher wind speeds tend to shift from the ocean's direction to the mainland's and *vice versa*. In South Jakarta (SJ), the

prevailing wind direction is from the mountainous area into Jakarta, occasionally bringing volcanic emissions as a unique natural source for the Jakarta area. Additionally, the CBPFs, a key tool in our research, have detected the possibility of pollutants transport, particularly sulphur, from Central to the North and South Jakarta during higher wind speeds. The CBPFs completed and enhanced the results for the source identification.

Black carbon (BC) and sulphur (S) majorly contribute to fine particles at all locations. However, the study found more detailed information on source diversity in each location. In CJ, which exhibited the highest concentrations, BC correlated strongly with road dust emissions. Sulphur was grouped with Cr and Ni in another factor, indicating a mixture of vehicle emission and tire-and-brake wear. The two factors serve as confirmation of heavily congested traffic in CJ. The dense traffic with a very high percentage of calm wind (>80%) signifies that the sources are local. In contrast, open waste and biomass burning were the likely sources of BC, K, and Cl in SJ. In NJ, fine BC particles tended to come from the west-northwest, like various metal elements, suggesting industrial sources, including those located in neighbouring cities. CBPFs of the coarse particles identified S of different source types coming from the direction of the port in the northeast. At the same time, commuting traffic and industrial activities towards the northwest could be a significant source of BC contributors.

The results of our study not only inform but also call for action that local governments can implement. The fuel production process at oil refineries, a key stage in lowering the sulphur content in fuel, is influenced by the decisions of various stakeholders at higher levels. However, several significant particulate elements can be reduced locally. Sulphur can be minimised through measures that encourage fuel consumption reduction. Decongestion will concurrently reduce tire-and-brake wear of toxic metals, especially in the Central and North Jakarta areas. These policy options can also simultaneously decrease the concentration of traffic-related BC. Efforts to lessen BC in SJ must focus on monitoring and preventing the open burning of waste. The potential impact of these policy actions is significant, inspiring all stakeholders to take immediate and effective measures.

The natural sources of marine and less-known volcanic activity can contribute to the background concentration in many countries and regions with unique geography, being in proximity to the sea and volcanoes. The local air quality management plan of these countries needs to carefully consider these natural sources when defining the PM10 background level and reduction targets, as well as the future ambient air quality standard.

The results of this study underscore the importance of regularly monitoring chemical composition and continuously measuring fine and coarse particulates in various locations. This continuous monitoring is crucial for maintaining the effectiveness of air quality management policies and ensuring the health and well-being of the population. Further information can be gained through the refinement of the particulate composition by adding other chemical parameters that have not been analysed in this study. More comprehensive composition analysis will add to source identification and help improve air quality management policies.

Author contributions

D: conceptualization, funding acquisition, methodology, resource management, supervision, rewriting and editing of the final manuscript; NKS: data curation, formal analysis, investigation, visualization, and writing the original manuscript; MS: methodology, supervision, validation, and review of the manuscript; DDL: methodology, resource management, validation.

Conflicts of interest

There are no conflicts of interest to declare.

Data availability

The data supporting this article have been included as part of the supplementary information (SI). Supplementary information: measurement data for elemental fine and coarse particles, statistical analysis results not included in the main article, and the Hysplit ash cloud dispersion modelling result. See DOI: **https://doi.org/10.1039/d5ea00059a**.

Acknowledgements

The research is a part of the UDARA project funded by Lembaga Pengelola Dana Pendidikan (LPDP) under Dana Ilmu Pengetahuan Indonesia (DIPI) on the work scheme of DIPI-UK (PI Dr Driejana) in collaboration with the University of Manchester (PI Prof. G. McFiggans), No. 1030/I1.CO9/PN-DN/2019, administrated by the Faculty of Civil and Environmental Engineering, Institut Teknologi Bandung. We gratefully acknowledge the Jakarta Province Environmental Agency (DLH-DKI) for providing meteorological data and the National Research and Innovation Agency of Indonesia (BRIN) (previously BATAN)) for sampling equipment and analytical instruments.

References

1 WHO, *Sixty-eight World Health Assembly*, 2015.
2 A. J. Cohen, M. Brauer, R. Burnett, H. R. Anderson, J. Frostad, K. Estep, K. Balakrishnan, B. Brunekreef, L. Dandona, R. Dandona, V. Feigin, G. Freedman, B. Hubbell, A. Jobling, H. Kan, L. Knibbs, Y. Liu, R. Martin, L. Morawska, C. A. Pope, H. Shin, K. Straif, G. Shaddick, M. Thomas, R. Van Dingenen, A. Van Donkelaar, T. Vos, C. J. L. Murray and M. H. Forouzanfar, Estimates and 25-year trends of the global burden of disease attributable to ambient air pollution: an analysis of data from the Global Burden of Diseases Study 2015, *Lancet*, 2017, **389**, 1907–1918.
3 M. Manousakas, K. Eleftheriadis and H. Papaefthymiou, Characterization of PM10 Sources and Ambient Air Concentration Levels at Megalopolis City (Southern Greece)

Located in the Vicinity of Lignite-Fired Plants, *Aerosol Air Qual. Res.*, 2013, **13**, 804–817.
4 S. Gautam, A. Yadav, C.-J. Tsai and P. Kumar, A review on recent progress in observations, sources, classification and regulations of PM2.5 in Asian environments, *Environ. Sci. Pollut. Res.*, 2016, **23**, 21165–21175.
5 D. A. Vallero, *Fundamentals of Air Pollution*, Elsevier, Amsterdam, 4th edn, 2008.
6 WHO, World health statistics 2012, *Statistiques Sanitaires Mondiales 2012*, 2012, p. 176.
7 S. A. Meo, A. N. Memon, S. A. Sheikh, F. A. Rouq, A. M. Usmani, A. Hassan and S. A. Arian, Effect of environmental air pollution on type 2 diabetes mellitus, *Eur. Rev. Med. Pharmacol. Sci.*, 2015, **19**, 123–128.
8 A. Mutlu, B.-K. Lee, G.-H. Park, B.-G. Yu and C.-H. Lee, Long-term concentrations of airborne cadmium in metropolitan cities in Korea and potential health risks, *Atmos. Environ.*, 2012, **47**, 164–173.
9 P. H. N. Saldiva, R. W. Clarke, B. A. Coull, R. C. Stearns, J. Lawrence, G. G. K. Murthy, E. Diaz, P. Koutrakis, H. Suh, A. Tsuda and J. J. Godleski, Lung Inflammation Induced by Concentrated Ambient Air Particles Is Related to Particle Composition, *Am. J. Respir. Crit. Care Med.*, 2002, **165**, 1610–1617.
10 M. Amalia, B. P. Resosudarmo and J. Bennett, The Consequences of Urban Air Pollution For Child Health: What Does Self-Reporting Data In The Jakarta Metropolitan Area Reveal?.
11 E. Aldrian and R. Dwi Susanto, Identification of three dominant rainfall regions within Indonesia and their relationship to sea surface temperature, *Int. J. Climatol.*, 2003, **23**, 1435–1452.
12 M. D. Syaifullah, Analisis Kondisi Udara Atas Wilayah Indonesia dengan Data Radiosonde, *Jurnal Meteorologi dan Geofisika*, 2018, **18**(1), DOI: **10.31172/jmg.v18i1.268**.
13 B. DKI Jakarta Province, DKI Jakarta Province in Figures 2019, *BPS Statistics-DKI Jakarta*, Jakarta, 2019.
14 BPS, *Statistical Yearbook of Indonesia, Badan Pusat Statistik (BPS-Statistics Indonesia)*, Jakarta, 2019th edn, 2019.
15 M. Santoso, D. D. Lestiani and A. Markwitz, Characterization of airborne particulate matter collected at Jakarta roadside of an arterial road, *J. Radioanal. Nucl. Chem.*, 2013, **297**, 165–169.
16 M. Santoso, D. Dwiana Lestiani and P. K. Hopke, Atmospheric black carbon in $PM_{2.5}$ in Indonesian cities, *J. Air Waste Manage. Assoc.*, 2013, **63**, 1022–1025.
17 M. Santoso, D. D. Lestiani, E. Damastuti, S. Kurniawati, I. Kusmartini, D. P. Dwi Atmodjo, D. K. Sari, T. Muhtarom, D. A. Permadi and P. K. Hopke, Long term characteristics of atmospheric particulate matter and compositions in Jakarta, Indonesia, *Atmos. Pollut. Res.*, 2020, **11**, 2215–2225.
18 S. D. A. Kusumaningtyas, E. Aldrian, T. Wati, D. Atmoko and S. Sunaryo, The Recent State of Ambient Air Quality in Jakarta, *Aerosol Air Qual. Res.*, 2018, **18**, 2343–2354.
19 P. Lestari, M. K. Arrohman, S. Damayanti and Z. Klimont, Emissions and spatial distribution of air pollutants from anthropogenic sources in Jakarta, *Atmos. Pollut. Res.*, 2022, **13**, 101521.
20 G. Syuhada, A. Akbar, D. Hardiawan, V. Pun, A. Darmawan, S. H. A. Heryati, A. Y. M. Siregar, R. R. Kusuma, R. Driejana, V. Ingole, D. Kass and S. Mehta, Impacts of Air Pollution on Health and Cost of Illness in Jakarta, Indonesia, *IJERPH*, 2023, **20**, 2916.
21 USEPA, *Final Regulatory Impact Analysis for the Reconsideration of the National Ambient Air Quality Standards for Particulate Matter*, EPA-452/R-24-006, January 2024.
22 R. Byrne, K. Ryan, D. S. Venables, J. C. Wenger and S. Hellebust, Highly local sources and large spatial variations in $PM_{2.5}$ across a city: evidence from a city-wide sensor network in Cork, Ireland, *Environ. Sci.: Atmos.*, 2023, **3**, 919–930.
23 J. P. Pinto, A. S. Lefohn and D. S. Shadwick, Spatial Variability of $PM_{2.5}$ in Urban Areas in the United States, *J. Air Waste Manage. Assoc.*, 2004, **54**, 440–449.
24 P. K. Hopke, Y. Xie, T. Raunemaa, S. Biegalski, S. Landsberger, W. Maenhaut, P. Artaxo and D. Cohen, Characterization of the Gent Stacked Filter Unit PM_{10} Sampler, *Aerosol Sci. Technol.*, 1997, **27**, 726–735.
25 B. A. Begum and P. K. Hopke, Identification of Sources from Chemical Characterization of Fine Particulate Matter and Assessment of Ambient Air Quality in Dhaka, Bangladesh, *Aerosol Air Qual. Res.*, 2019, **19**, 118–128.
26 S. K. Biswas, S. A. Tarafdar, A. Islam, M. Khaliquzzaman, H. Tervahattu and K. Kupiainen, Impact of Unleaded Gasoline Introduction on the Concentration of Lead in the Air of Dhaka, Bangladesh, *J. Air Waste Manage. Assoc.*, 2003, **53**, 1355–1362.
27 M. Santoso and D. D. Lestiani, *X-ray Fluorescence in Member States (Indonesia): Application of ED XRF in Supporting National Program of Air Quality Improvement in Indonesia*, IAEA, 2014, pp. 8–14.
28 D. K. Sari, D. D. Lestiani, S. Kurniawati, N. Adventini, D. P. D. Atmodjo and I. Kusmartini, Applicability of EDXRF for elemental analysis in airborne particulate matter (APM): assessment using APM reference material, *J. Phys.: Conf. Ser.*, 2020, **1436**, 012137.
29 A. Reff, S. I. Eberly and P. V. Bhave, Receptor Modeling of Ambient Particulate Matter Data Using Positive Matrix Factorization: Review of Existing Methods, *J. Air Waste Manage. Assoc.*, 2007, **57**, 146–154.
30 D. C. Carslaw and K. Ropkins, openair — An R package for air quality data analysis, *Environ. Model. Softw.*, 2012, **27–28**, 52–61.
31 X. Zhou, Z. Cao, Y. Ma, L. Wang, R. Wu and W. Wang, Concentrations, correlations and chemical species of PM2.5/PM10 based on published data in China: potential implications for the revised particulate standard, *Chemosphere*, 2016, **144**, 518–526.
32 *Urban Airborne Particulate Matter: Origin, Chemistry, Fate and Health Impacts*, ed. F. Zereini and C. L. S. Wiseman, Springer Berlin Heidelberg, Berlin, Heidelberg, 2011.

33 G. D. Thurston, K. Ito and R. Lall, A source apportionment of U.S. fine particulate matter air pollution, *Atmos. Environ.*, 2011, **45**, 3924–3936.
34 J. C. Chow, D. H. Lowenthal, L.-W. A. Chen, X. Wang and J. G. Watson, Mass reconstruction methods for PM2.5: a review, *Air Qual. Atmos. Health*, 2015, **8**, 243–263.
35 W. C. Malm, J. F. Sisler, D. Huffman, R. A. Eldred and T. A. Cahill, Spatial and seasonal trends in particle concentration and optical extinction in the United States, *J. Geophys. Res.*, 1994, **99**, 1347–1370.
36 N. Siddique and S. Waheed, Source apportionment using reconstructed mass calculations, *J. Environ. Sci. Health, Part A*, 2014, **49**, 463–477.
37 J. G. Watson, J. C. Chow, D. H. Lowenthal, L.-W. A. Chen and X. Wang, *Reformulation of PM 2.5 Mass Reconstruction Assumptions for the San Joaquin Valley*, Desert Research Institute, 2012.
38 W. Maenhaut, F. François, J. Cafmeyer and O. Okunade, Size-fractionated aerosol composition at Gent, Belgium. Results from a one-year study, *Nucl. Instrum. Methods Phys. Res., Sect. B*, 1996, **109–110**, 476–481.
39 J. P. Riley and R. Chester, *Introduction to Marine Chemistry*, Academic Press, London, New York, 1971.
40 X. Zhu, *Investigation of Aerosol Optical and Chemical Properties Using Humidity Controlled Cavity Ring-Down Spectroscopy*, 2000.
41 A. Jeričević, G. Gašparac, M. M. Mikulec, P. Kumar and M. T. Prtenjak, Identification of diverse air pollution sources in a complex urban area of Croatia, *J. Environ. Manage.*, 2019, **243**, 67–77.
42 M. Masiol, S. Squizzato, M.-D. Cheng, D. Q. Rich and P. K. Hopke, Differential Probability Functions for Investigating Long-term Changes in Local and Regional Air Pollution Sources, *Aerosol Air Qual. Res.*, 2019, **19**, 724–736.
43 A. Mukherjee and M. Agrawal, Assessment of local and distant sources of urban PM2.5 in middle Indo-Gangetic plain of India using statistical modeling, *Atmos. Res.*, 2018, **213**, 275–287.
44 I. Uria-Tellaetxe and D. C. Carslaw, Conditional bivariate probability function for source identification, *Environ. Model. Softw.*, 2014, **59**, 1–9.
45 J. H. Seinfeld and S. N. Pandis, *Atmospheric Chemistry and Physics: from Air Pollution to Climate Change*, Wiley-Interscience, s.l., 2. Aufl., 2012.
46 C. Pio, C. Alves, T. Nunes, M. Cerqueira, F. Lucarelli, S. Nava, G. Calzolai, V. Gianelle, C. Colombi, F. Amato, A. Karanasiou and X. Querol, Source apportionment of PM2.5 and PM10 by Ionic and Mass Balance (IMB) in a traffic-influenced urban atmosphere, in Portugal, *Atmos. Environ.*, 2020, **223**, 117217.
47 J. Cyrys, J. Heinrich, G. Hoek, K. Meliefste, M. Lewné, U. Gehring, T. Bellander, P. Fischer, P. V. Vliet, M. Brauer, H.-E. Wichmann and B. Brunekreef, Comparison between different traffic-related particle indicators: elemental carbon (EC), PM2.5 mass, and absorbance, *J. Exposure Sci. Environ. Epidemiol.*, 2003, **13**, 134–143.
48 M. Evans, N. Kholod, T. Kuklinski, A. Denysenko, S. J. Smith, A. Staniszewski, W. M. Hao, L. Liu and T. C. Bond, Black carbon emissions in Russia: a critical review, *Atmos. Environ.*, 2017, **163**, 9–21.
49 S. Waheed, N. Siddique, M. Arif, M. Daud and A. Markwitz, Size-fractionated airborne particulate matter characterization of a residential area near Islamabad airport by IBA methods, *J. Radioanal. Nucl. Chem.*, 2012, **293**, 279–287.
50 D. D. Cohen, J. Crawford, E. Stelcer and V. T. Bac, Characterisation and source apportionment of fine particulate sources at Hanoi from 2001 to 2008, *Atmos. Environ.*, 2010, **44**, 320–328.
51 WHO, *WHO Global Air Quality Guidelines: Particulate Matter (PM2. 5 and PM10), Ozone, Nitrogen Dioxide, Sulfur Dioxide and Carbon Monoxide*, World Health Organization, Geneva, 1st edn, 2021.
52 C. A. Pope and D. W. Dockery, Health Effects of Fine Particulate Air Pollution: Lines that Connect, *J. Air Waste Manage. Assoc.*, 2006, **56**, 709–742.
53 E. Kim and P. K. Hopke, Source characterization of ambient fine particles at multiple sites in the Seattle area, *Atmos. Environ.*, 2008, **42**, 6047–6056.
54 C. M. Long, M. A. Nascarella and P. A. Valberg, Carbon black *vs.* black carbon and other airborne materials containing elemental carbon: physical and chemical distinctions, *Environ. Pollut.*, 2013, **181**, 271–286.
55 M. Z. Jacobson, Control of fossil-fuel particulate black carbon and organic matter, possibly the most effective method of slowing global warming, *J. Geophys. Res.*, 2002, **107**(D19), ACH 16-1–ACH 16-22.
56 Republik Indonesia, *Peraturan Menteri Lingkungan Hidup Dan Kehutanan Nomor P.20/menlhk/setjen/kum.1/3/2017 Tahun 2017 Tentang Baku Mutu Emisi Gas Buang Kendaraan Bermotor Tipe Baru Kategori M, Kategori N, Dan Kategori O*, 2017.
57 T. Jayasekher, Aerosols near by a coal fired thermal power plant: chemical composition and toxic evaluation, *Chemosphere*, 2009, **75**, 1525–1530.
58 Y. Kang, G. Liu, C.-L. Chou, M. H. Wong, L. Zheng and R. Ding, Arsenic in Chinese coals: distribution, modes of occurrence, and environmental effects, *Sci. Total Environ.*, 2011, **412–413**, 1–13.
59 M. Viana, T. A. J. Kuhlbusch, X. Querol, A. Alastuey, R. M. Harrison, P. K. Hopke, W. Winiwarter, M. Vallius, S. Szidat, A. S. H. Prévôt, C. Hueglin, H. Bloemen, P. Wåhlin, R. Vecchi, A. I. Miranda, A. Kasper-Giebl, W. Maenhaut and R. Hitzenberger, Source apportionment of particulate matter in Europe: a review of methods and results, *J. Aerosol Sci.*, 2008, **39**, 827–849.
60 Z. Farahmandkia, F. Moattar, F. Zayeri, M. Sadegh Sekhavatjou and N. Mansouri, Contribution of point and small-scaled sources to the PM10 emission using positive matrix factorization model, *J. Environ. Health Sci. Eng.*, 2017, **15**, 2.
61 L. O. Mbeng, J. Probert, P. S. Phillips and R. Fairweather, Assessing Public Attitudes and Behaviour to Household Waste Management in Cameroon to Drive Strategy

Development: A Q Methodological Approach, *Sustainability*, 2009, **1**, 556–572.
62 A. Ooki, M. Uematsu, K. Miura and S. Nakae, Sources of sodium in atmospheric fine particles, *Atmos. Environ.*, 2002, **36**, 4367–4374.
63 S. Vassilev, Contents, modes of occurrence and behaviour of chlorine and bromine in combustion wastes from coal-fired power stations, *Fuel*, 2000, **79**, 923–938.
64 H.-G. Ni, S.-Y. Lu, T. Mo and H. Zeng, Brominated flame retardant emissions from the open burning of five plastic wastes and implications for environmental exposure in China, *Environ. Pollut.*, 2016, **214**, 70–76.
65 P. Svobodová, S. R. Jílková, J. Kohoutek, O. Audy, P. Šenk and L. Melymuk, High levels of flame retardants in vehicle dust indicate ongoing use of brominated and organophosphate flame retardants in vehicle interiors, *Environ. Monit. Assess.*, 2025, **197**(4), 396.
66 X. Wu, Q. Kong, Y. Lan, J. Sng and L. E. Yu, Refined Sea Salt Markers for Coastal Cities Facilitating Quantification of Aerosol Aging and $PM_{2.5}$ Apportionment, *Environ. Sci. Technol.*, 2024, **58**, 8432–8443.
67 H. M. Ten Brink, Reactive uptake of HNO3 and H2SO4 in sea-salt (NaCl) particles, *J. Aerosol Sci.*, 1998, **29**, 57–64.
68 Y. Zhang, R. Han, G. Wu, X. Wang, L. Li, M. Li, Z. Zhou, J. Z. Yu and Y. Zhou, Improved method for estimating chlorine depletion in sea salt aerosols using single particle aerosol mass spectrometer, *Atmos. Environ.*, 2025, **353**, 121243.
69 A. L. Bondy, B. Wang, A. Laskin, R. L. Craig, M. V. Nhliziyo, S. B. Bertman, K. A. Pratt, P. B. Shepson and A. P. Ault, Inland Sea Spray Aerosol Transport and Incomplete Chloride Depletion: Varying Degrees of Reactive Processing Observed during SOAS, *Environ. Sci. Technol.*, 2017, **51**, 9533–9542.
70 S. K. Hassan, A. A. El-Abssawy and M. I. Khoder, Characteristics of gas–phase nitric acid and ammonium–nitrate– sulfate aerosol, and their gas–phase precursors in a suburban area in Cairo, Egypt, *Atmos. Pollut. Res.*, 2013, **4**, 117–129.
71 I. Wesley and T. Whiley, *Better Brakes Baseline Report*, Department of Ecology State of Washington (Publication No. 13-04-010), 2013.
72 G. Grivas, S. Cheristanidis, A. Chaloulakou, P. Koutrakis and N. Mihalopoulos, Elemental Composition and Source Apportionment of Fine and Coarse Particles at Traffic and Urban Background Locations in Athens, Greece, *Aerosol Air Qual. Res.*, 2018, **18**, 1642–1659.
73 G. Wang, P. K. Hopke and J. R. Turner, Using highly time resolved fine particulate compositions to find particle sources in St. Louis, MO, *Atmos. Pollut. Res.*, 2011, **2**, 219–230.
74 *Global Volcanism Program*, Smithsonian Institute, National Museum of Natural History, 2025.
75 R. A. Mihai, I. A. Espinoza-Caiza, E. J. Melo-Heras, N. S. Cubi-Insuaste, E. A. Pinto-Valdiviezo and R. D. Catana, Does the Mineral Composition of Volcanic Ashes Have a Beneficial or Detrimental Impact on the Soils and Cultivated Crops of Ecuador?, *Toxics*, 2023, **11**, 846.
76 J. Martínez-Martínez, J. F. Mediato, M. P. Mata, B. Ordóñez, B. Del Moral, E. Bellido, R. Pérez-López, M. A. Rodríguez-Pascua, J. Vegas, G. Lozano Otero, R. M. Mateos, N. Sánchez and I. Galindo, Early fumarolic minerals from the Tajogaite volcanic eruption (La Palma, 2021), *J. Volcanol. Geotherm. Res.*, 2023, **435**, 107771.
77 R. W. Birnie and J. H. Hall, The geochemistry of El Misti volcano, Peru fumaroles, *Bull. Volcanol.*, 1974, **38**, 1–15.
78 A. Gutmann, N. Bobrowski, T. J. Roberts, J. Rüdiger and T. Hoffmann, Advances in Bromine Speciation in Volcanic Plumes, *Front. Earth Sci.*, 2018, **6**, 213.
79 A. Aiuppa, C. Federico, A. Franco, G. Giudice, S. Gurrieri, S. Inguaggiato, M. Liuzzo, A. J. S. McGonigle and M. Valenza, Emission of bromine and iodine from Mount Etna volcano, *Geochem., Geophys., Geosyst.*, 2005, **6**, 2005GC000965.
80 *READY HYSPLIT Dispersion Model*, **https://www.ready.noaa.gov/hypub-bin/dispasrc.pl**, accessed 7 July 2025.